INVESTIGATING THE MOTILITY OF PLASMODIUM

by
Natasha Vartak

A thesis submitted to Johns Hopkins University in conformity with the requirements for the degree of Master of Science

Baltimore, Maryland
April, 2017

ABSTRACT

Malaria is a life-threatening disease and the search for vaccine targets to the malaria parasite *Plasmodium* continues to be of utmost importance. Antibody mediated vaccines to the pre-erythrocytic stage of *Plasmodium* represent the best opportunity for vaccine development due to the potential to stop or decrease the number of sporozoites that reach the liver and trigger symptomatic disease. *Plasmodium* sporozoites are actively motile and this motility is critical to their infectivity. Inhibition of gliding has been used to assess whether particular surface proteins of the sporozoite good vaccine targets. We present a method that can be used to assess antibody mediated inhibition of gliding motility by quantifying the fluorescence intensity of the trails that sporozoites leave behind as they move. We demonstrate the functionality of the assay with the human malaria parasite *Plasmodium falciparum* and a known inhibitory monoclonal antibody 2A10. Our data suggests that the fluorescence intensity assay can be a useful in vitro method of assessing the efficacy of antigen based vaccines. *Plasmodium* surface proteins thrombospondin-related anonymous protein (TRAP) and circumsporozoite protein (CSP) play important roles in sporozoite motility. CSP is the basis of the RTS,S malaria vaccine but the relationship between TRAP and CSP has yet to be fully illuminated. We investigated the distribution of TRAP on the surface of wild type and *Plasmodium berghei* CSP repeat mutant sporozoites in gliding and non-gliding conditions. Our data suggests that there is a correlation between irregular gliding motility and decreased secretion of TRAP.

Thesis advisor – Dr. Photini Sinnis.

Secondary reader – Dr. Fidel Zavala

ACKNOWLEDGEMENTS

I am grateful to Dr. Photini Sinnis whose mentorship and expertise have allowed me to fully immerse myself in my research. She gave me the freedom to tailor a thesis project to my interests and I am a better scientist because of her guidance.

I would like to thank Dr. Fidel Zavala for generously agreeing to review my thesis and his insights into my project. Amanda Balaban, my student mentor over the past year, has played a large role in my success in the lab. Her mentorship gave me the confidence to work independently in the lab and her advice helped me craft this thesis. I am grateful to have known and worked with my Sinnis Lab colleagues Dr. Melanie Shears and Gibbs Nasir. Our triumph in the Halloween Costume Contest of 2016 is a particularly fond memory of mine. I would also like to thank Dr. Godfree Mlambo, Dr Abhay Tripathi, and Chris Kizito. None of the work I have done in this thesis would be possible without their help in providing mosquitoes and parasites. I would like to thank my friends Nikita Shah, Brooke Pearlman, Suraj Uttamchandani, and Jessica Morris who have kept me grounded during my time in college and graduate school.

Thank you to my aunt Dr. Sangeeta Gajendra who has supported me over the past six years of my academic career. Most of all, I would like to thank my mother Dr. Divyangana Vartak, without whom I would not be able to pursue my dream of studying in the United States. Although we are separated by thousands of miles of oceans, you are always with me and you are my constant source of inspiration and strength.

TABLE OF CONTENTS

LIST OF TABLES

LIST OF FIGURES

INTRODUCTION

Malaria continues to be a life-threatening disease worldwide, causing approximately 600,000 deaths and 200 million cases [10]. Malaria belongs to the genus *Plasmodium* and is caused by apicomplexan parasites that complete their life cycle in both mosquito and vertebrate hosts [4]. *Plasmodium falciparum* causes the largest number of fatal diseases but other species also play a role in illness including *P. vivax, P. ovale curtisi, P. ovale wallikeri, P. malariae,* and *P. knowlesi* [10]. In rodents, malaria species include *P. berghei, P. yoelli, P. chabaudi, and P. vinckei.*

The malaria life cycle begins when an *Anopheles* mosquito bites a vertebrate hosts and takes a blood meal [10]. In doing so, the mosquito ingests *Plasmodium* gametocytes which then form gametes [3]. In the midgut of the mosquito, the female and male gametes fuse to form a fertilized zygote called an ookinete [3]. Ookinetes are motile and they invade the mosquito midgut and form oocysts [3]. The oocysts enlarge and eventually rupture, releasing the infectious stage of *Plasmodium* called sporozoites [12]. Sporozoites mature and invade the salivary glands of the mosquito where they are ready to be transmitted to another vertebrate host [12]. Transmission of sporozoites occurs when the mosquito probes the skin of the host with its proboscis looking for blood [3]. This probing causes sporozoites in mosquito saliva to be injected into the skin [12, 28, 31]. Once in the skin, sporozoites carry out a form of motion called gliding motility and invade blood vessels [4, 14]. Sporozoites in the blood are carried to the liver where they invade hepatocytes [3].

Once *Plasmodium* has infected the liver, sporozoites develop into the exoerythocytic form of the parasite called schizonts [3]. Schizonts rupture and release thousands of

merozoites that invade erythrocytes [10]. In the red blood cells, merozoites develop into trophozoites which then form schizonts [10]. The release of merozoites and infection of red blood cells is cyclical, causing a large increase in parasite load [3]. This blood stage of infection causes clinical manifestations of malaria [10]. Merozoites form gametocytes that can then be ingested by more mosquitoes, continuing the spread of the parasite [10]. Our best chance at stopping the progression of malaria is preventing sporozoite invasion and traversal. Not only are there lower numbers of parasites at this stage but targeting invasion and traversal prevents the development and release of merozoites; this means that the blood stage of infection and potential life-threatening clinical disease are not given the opportunity to manifest.

The only malaria vaccine that has shown potential in Phase III clinical trials is RTS,S, a pre-erythrocytic stage vaccine that targets circumsporozoite protein (CSP) on the surface of sporozoites [18]. CSP coats the entire surface of the sporozoite and is made up of an NH_2-terminal domain, a central repeat region, and a C terminal thrombospondin repeat (TSR) [19]. The RTS,S vaccine is a fusion protein consisting of the CSP repeat region and the TSR adhesive domain fused to the surface antigen of hepatitis B [22]. The RTS,S vaccine induces an antibody response and has shown promise in protection against *P. falciparum* but this protection is not long lasting. In a phase III randomized, controlled trial conducted at 11 locations in Africa, young infants and children were administered 3 doses of either RTS,S/AS01 or a control vaccine [22]. Vaccine efficacy against clinical malaria (including severe disease or disease requiring hospitalization) was tracked for 18 months post immunization. Vaccine efficacy in children was shown to be 46% during the 18

months of the trial. Efficacy against severe disease or malaria hospitalization decreased to 34% and 19% respectively during the 20th month post immunization [22]. Vaccine efficacy against clinical malaria was 27% in young infants [22], and even with a lower efficacy, a number of clinical malaria cases were avoided due to immunization, there was no significant protection against severe malaria or hospitalization [22]. Importantly, vaccine efficacy decreased over time for both children and young infants [22]. Therefore, although RTS,S is the gold standard for malaria vaccines, the search for other antigen targets to enhance the RTS,S vaccine continues. The PATH Malaria Vaccine Initiative's HPATIC project, which our results contribute to, is a hypothesis-driven approach to finding non-CSP sporozoite vaccine targets.

While the structure and function of CSP have been studied [8, 9, 19, 21], as of yet the exact role of the repeats is yet to be fully illuminated. A previous study has shown that mutant parasites that lack the repeat region are unable to produce functional sporozoites [13]. Since the deletion of the entire repeat sequence gives rise to a severe phenotype, our lab has generated CSP repeat mutants that allow sporozoites to develop but show different motility phenotypes than wild type parasites. Since CSP is shed as parasites move and TRAP has been shown to be necessary for gliding motility [11, 26], the relationship between CSP and TRAP in mutant parasites is of great interest. Here we explore the role of TRAP in these CSP repeat mutant parasites as it applies to sporozoite gliding motility.

GLIDING MOTILITY IN PLASMODIUM FALCIPARUM

INTRODUCTION

The PATH Malaria Vaccine Initiative HPATIC project began as a hypothesis driven approach to finding a pre-erythocytic stage vaccine for *Plasmodium falciparum*. A consortium of laboratories from Johns Hopkins University (JHU), the Center for Infectious Disease Research (CIDR), the Walter Reed Army Institute of Research (WRAIR), the National Institutes of Health (NIH), and the Naval Medical Research Center (NMRC) came together to determine the antigen candidates for vaccine development. 64 antigens were chosen by the consortium on a range of criteria that included biological rationale, observed in vivo protection in rodents, functional assay activity, sporozoite surface expression, putative functional domains, and human sera reactivity. Out of these 64 antigens, 24 were prioritized based on characteristics that would make them good vaccine targets (Fig. 1). Antigens that demonstrated multiple characteristics were of the highest priority (Fig. 1.).

23 of the 24 antigens were expressed in vitro using a wheat germ system [23]. The 24th antigen was broken up and 2 domains were expressed independently. Balb/c mice were immunized with the wheat germ antigens and polyclonal antibodies were obtained (Fig. 2). These antibodies were blinded and designated to random HEPA groups before being tested in multiple functional assays. These functional assays were performed by the labs that chosen the initial antigen vaccine candidates. JHU performed ELISA, permeabilized and live IFAs, and gliding motility assays. Invasion and traversal assays were carried out at

CIDR and ILSDA was performed by NMRC. Polyclonal antibodies that showed positive results in multiple functional assays were prioritized for the next stage of testing.

The next stage involved making monoclonal antibodies in Kymice using the proteins that produced antibodies with activity in the above mentioned assays (Fig. 2). Kymice are transgenic and while their antibody genes have mouse constant regions, the variable regions have been replaced by the complete human immunoglobulin genes from three loci [29] so they produce humanized antibodies. –

In order to prioritize the mAbs to be tested, Atreca technology was used to sequence antibody genes [1]. Atreca sequences antibody heavy and light chains using next generation sequencing (NGS) and DNA barcoding [1]. This 454 deep sequencing technology pairs heavy and light antibody chains that originate from single B cells and measures clonal evolution and clonal proportions [1]. From the library of mAbs generated, JHU received 118 antibodies from 11 different HEPA proteins for testing in gliding motility assays (Table 1).

The gliding motility assay has often been used to assess antibody-mediated vaccine efficacy [8]. In this assay, *P. falciparum* sporozoites are incubated with an inhibitory antibody then added to wells pre-coated with 2A10 and allowed to glide. The CSP trails shed by the sporozoites when gliding can be stained with an antibody against CSP and then observed under a fluorescent microscope. The ability of the inhibitory antibody to limit gliding is inversely correlated with the number of CSP trails [24]. In the classic assay, gliding motility is quantified by counting the number of sporozoites associated with trails

and the number of circles present in each trail [24]. However, there are limitations to the classic gliding motility assay; it can be both time consuming and low throughput, particularly when faced with the challenge of testing 118 monoclonal antibodies. Categorizing the trails can also be subjective and it can be difficult to differentiate between see small differences in motility. We set out to develop a medium throughput method for quantifying gliding motility that would be able to differentiate between subtle differences in of gliding that might otherwise be missed.

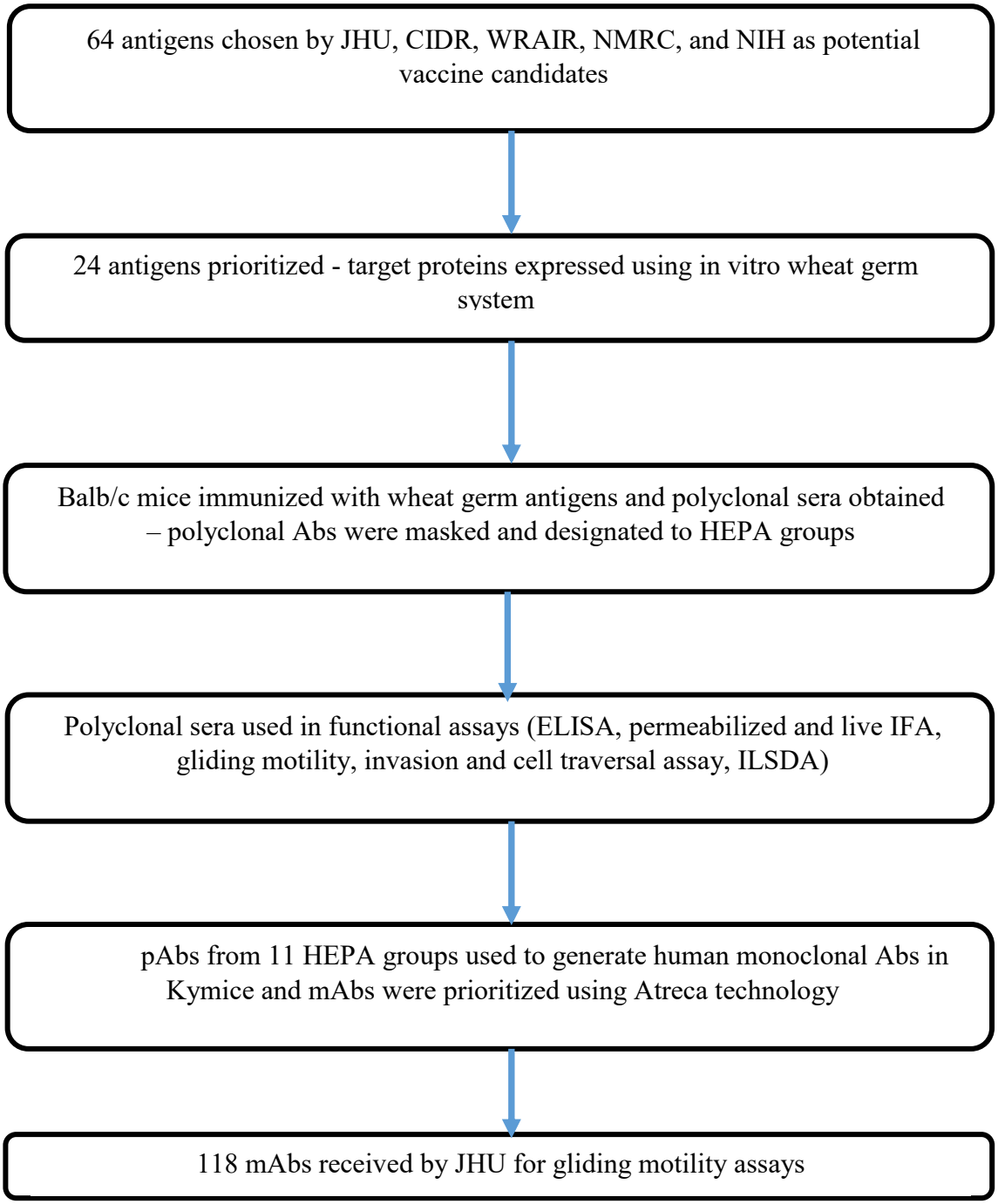

Figure 1. Overview of the HPATIC project.

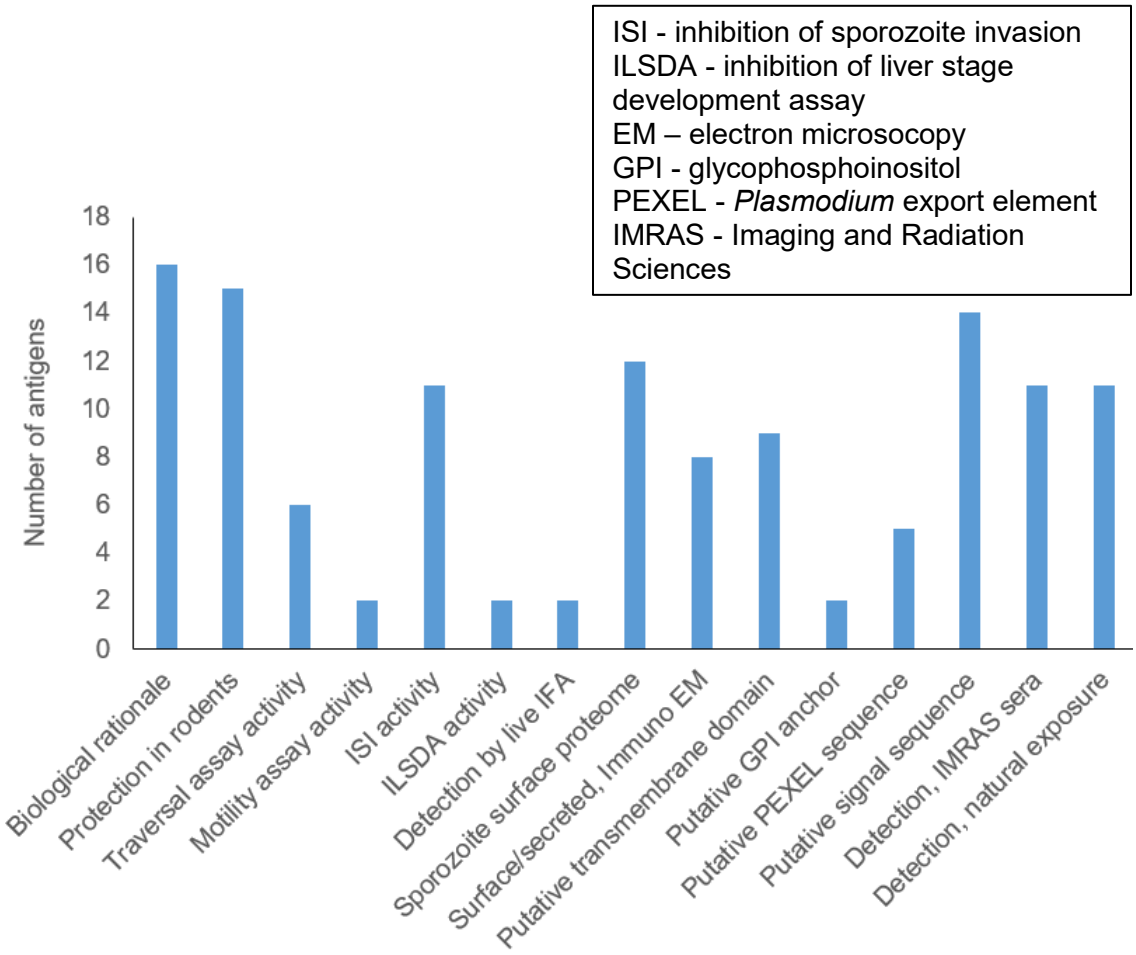

Figure 2. Characteristics of the top 24 HPATIC antigens.

HEPA antigen group	monoclonal antibodies
HEPA 103	1291, 1292, 1293, 1294, 1295, 1298, 1301, 1303, 1307, 1310, 1312, 1313, 1316, 1317, 1319, 1322, 1324, 1331, 1336, 1338
HEPA 106	1339, 1340, 1341, 1343, 1344, 1347, 1348, 1362, 1364, 1365, 1368, 1370, 1372, 1373, 1376, 1378, 1380, 1381, 1384, 1375, 1386
HEPA 112	1773, 1775, 1782, 1784, 1785, 1787, 1788, 1789, 1792, 1796, 1797, 1801, 1802 ,1803, 1804, 1806, 1811, 1812, 1813, 1817, 1818
HEPA 113	1822, 1833, 1834, 1838, 1841, 1842, 1858, 1961, 1864, 1865, 1866
HEPA 120	2260, 2265, 2278, 2280, 2283, 2289, 2293, 2300, 2304
HEPA 126	1873, 1874, 1875, 1876, 1890, 1897, 1899, 1901, 1905, 1908, 1909, 1910, 1914
HEPA 124	2308, 2318, 2320, 2321, 2325, 2326, 2329, 2339, 2340, 2341, 2342, 2347, 2348, 2349, 2350, 2351, 2354
HEPA 121	1919, 1935, 1936, 1937, 1938, 1948, 1950, 1951, 1955, 1957, 1958
HEPA 122	2204, 2206, 2207, 2211, 2213, 2216, 2220, 2221, 2224, 2227, 2229, 2231,2240, 2241, 2245
HEPA 109	2361, 2165, 2371, 2373, 2376, 2382, 2388, 2394, 2397, 2400, 2402
HEPA 125	2153, 2154, 2156, 2161, 2162, 2163, 2165, 216, 2167, 2169, 2169, 2171, 2174, 2175, 2176, 2178, 2179, 2182, 2194, 2196, 2198

Table 1. The monoclonal antibodies received by JHU for gliding motility assays split up according to the immunizing antigen.

METHODS

Mosquito rearing and production of sporozoites

NF54 gametocytes were used to produce *P. falciparum* sporozoites as described previously [29]. On day 16 post blood meal, sporozoites were isolated from mosquito salivary glands.

Methods for gliding motility assay

Glass coverslips were placed in a 24 well plate and coated with 10 µg/mL of 2A10 in 1x PBS pH 7.4 overnight at room temperature. Solutions with twice the desired inhibitory antibody concentration were made in 200 µL of 6% BSA/DMEM pH 7.4. The dilutions were made in 0.5mL Eppendorf tubes. Mosquitoes were dissected in DMEM (Dulbecco's Modified Eagle Medium) and sporozoites were isolated and counted. 200 µL containing 50000 sporozoites in DMEM were added to the previously made antibody dilution to get a final volume 400 µL of 3% BSA/DMEM per condition. The Eppendorf tubes containing sporozoites were incubated in a gradient thermocycler at 25°C for 30 minutes. Glass coverslips were washed 3 times with 1x PBS pH 7.4. Sporozoites were added to the washed coverslips and were spun for 4 minutes at 300g with an acceleration of 3 minutes and no brake deceleration. The 24 well plate was placed in a 5% CO2 incubator for 1 hour to allow sporozoites to glide. The media was removed from the well and the sporozoites were fixed with 4% paraformaldehyde for 1 hour at room temperature. The wells were washed 3 times with 1x PBS pH 7.4. The wells were blocked with

1%BSA/5% goat serum/BSA for 1 hour at 37°C. The wells were then stained with primary antibody for 1 hour at 37°C, washed 3 times with PBS, and then stained with secondary antibody for 1 hour at 37°C. The main primary antibody used was biotinylated 2A10 (1:100 dilution) followed by an Alexa fluor 488 conjugated streptavidin (1:500 dilution). The other primary used was an anti-C terminus of CSP antibody [16] (1:100 dilution) followed by a goat anti-rabbit IgG (H+L) highly cross adsorbed secondary conjugated to Alexa fluor 488 (1:500 dilution) [A-11034] . After staining, the wells were washed 3 times with PBS. The coverslips were carefully removed from the wells, allowed to dry for 10 minutes, and then mounted to slides with ProLong Gold antifade DAPI mounting media overnight. The coverslips were then sealed with clear nail polish and imaged using the 40x oil objective of a fluorescent microscope.

Fluorescence Intensity Assay

The parameters on the program Nikon NIS Basic Research Elements were set as follows: 40x nosepiece, 1280x1024 fast resolution, 1280x1024 16 bit quality, and high contrast. For the biotinylated 2A10 treated wells, the exposure time was 150ms. Due to increased background, the exposure time for the anti-C treated wells was 80 ms. 20 images spanning the entirety of the well were taken. To ensure random image acquisition, the microscope field of view was top to bottom on the left side of the well and 5 images were taken. The field of view was then moved to the right and 5 more images were taken. This process was repeated until 20 images were acquired. The sum fluorescence intensity from each image was collected using the ROI Statistics feature on NIS Elements.

Classic gliding motility assay

The number of sporozoites associated with trails was counted according to the following categories: 0 trails, 1-5 trails, 6-10 trails, 11-30 trails, and greater than 30 trails. Between 100 and 110 sporozoites were counted per coverslip.

Statistical analyses

To determine significance of results, unpaired T-tests were carried out with a 95% confidence interval

RESULTS

Development of fluorescence intensity assay

To address the limitations of the classic gliding motility assay, we developed a method that assessed gliding motility by quantifying the fluorescence intensity of the CSP trails (Fig. 3). The fluorescence intensity assay consisted of taking 20 images that spanned the coverslip in order to capture the diversity of trails present (Fig. 4). Using the ROI Statistics feature of the program NIS Elements, the sum fluorescence intensity of the CSP trails was collected.

First, we compared the classic assay to the fluorescence intensity assay using increasing concentrations of the inhibitory monoclonal antibody 2A10 (Fig. 5A and B). There is a significant difference in fluorescence intensity between 0 µg/mL and 5 µg/mL of 2A10 ($p<0.0001$) and between 5 µg/mL and 10 µg/mL of 2A10 ($p=0.0008$) (Fig. 5A). This suggests the marked decrease in fluorescence intensity as the concentration of 2A10 increases correlates with increased inhibition of gliding motility. To compare the fluorescence intensity data with the classic method, the same coverslips were viewed under a fluorescent microscope and the trails were counted (Fig. 5B). In the absence of an inhibitor almost 80% of the trails viewed contained more than 30 circles and as the concentration of 2A10 increased, the number of circles in the trails decreased showing inhibition of gliding (Fig. 5B). In order to test the sensitivity of the fluorescence intensity assay, another comparison of the two methods was carried out with lower concentrations of 2A10 (Fig. 6A). Using the classic method, once again the number of trails decreased as the concentration of 2A10 increased (Fig. 6B). Moreover, there is a significant difference

in fluorescence intensity between 0 µg/mL and 1 µg/mL of 2A10 ($p<0.0001$), 1µg/mL and 2.5 µg/mL ($p=0.002$), and between 2.5 µg/mL and 5 µg/mL of 2A10 ($p<0.0008$) (Fig. 6B). This suggests that not only does the fluorescence intensity assay correlate with the classic assay at lower concentrations of an inhibitory antibody but it is also sensitive enough to be able to significantly differentiate changes in inhibition that might not be detected by eye and enables better statistical analyses.

In order to confirm the effects of inhibition observed using 2A10, we carried out an experiment with cytochalasin D, an actin polymerization inhibitor that prevents motility [6] (Fig. 7A). When sporozoites were treated with cytochalasin D they could not glide and the low fluorescence intensity observed was due to the parasites being stained (Fig. 7A). The inhibition of fluorescence seen using cytochalasin D was comparable to the inhibition observed with 10µg/mL 2A10 (Fig. 7A). It is possible that the inhibition observed in our experiments was due to competition between the inhibitory 2A10 and the biotinylated 2A10 used to label the trails. Since they recognize the same epitope, the inhibitor may bind to CSP in the trails and obscure their labeling by biotinylated 2A10. In order to address this concern, we carried out a similar experiment using 2A10 as the inhibitory antibody but with a different detection antibody. The anti-C antibody we used detects the C terminal of CSP (Fig. 7B). Since a marked decrease in fluorescence intensity was still observed with a different detection antibody, we have greater confidence that the fluorescence intensity assay is able to correctly detect a decrease in gliding motility (Fig. 7B). Inhibition with 2A10 seems to be similar to inhibition with 2A10, however due to increased background in anti-C wells, a shorter exposure time is used when capturing images.

In order to look at the reproducibility of the fluorescence intensity assay, we carried out an experiment comparing the inhibition observed with untreated sporozoites, sporozoites treated with either human IgG or α-Pfs 25, and sporozoites treated with 2A10. Pfs 25 is a zygote/ookinete surface protein [27] and therefore the humanized mAb α-Pfs 25 should not show any inhibition of motility in *P. falciparum* sporozoites. Human IgG was also used as a negative control. We normalized the fluorescence intensity of α-Pfs 25 and 2A10 to the mean of the untreated control of each replicate (Fig. 8). Over 13 experiments, the assay seems to show strong consistency between experiments, giving us confidence in the reproducibility of the data. Hence, we decided to proceed with using the fluorescence intensity assay to test the human monoclonal antibodies provided by PATH MVI.

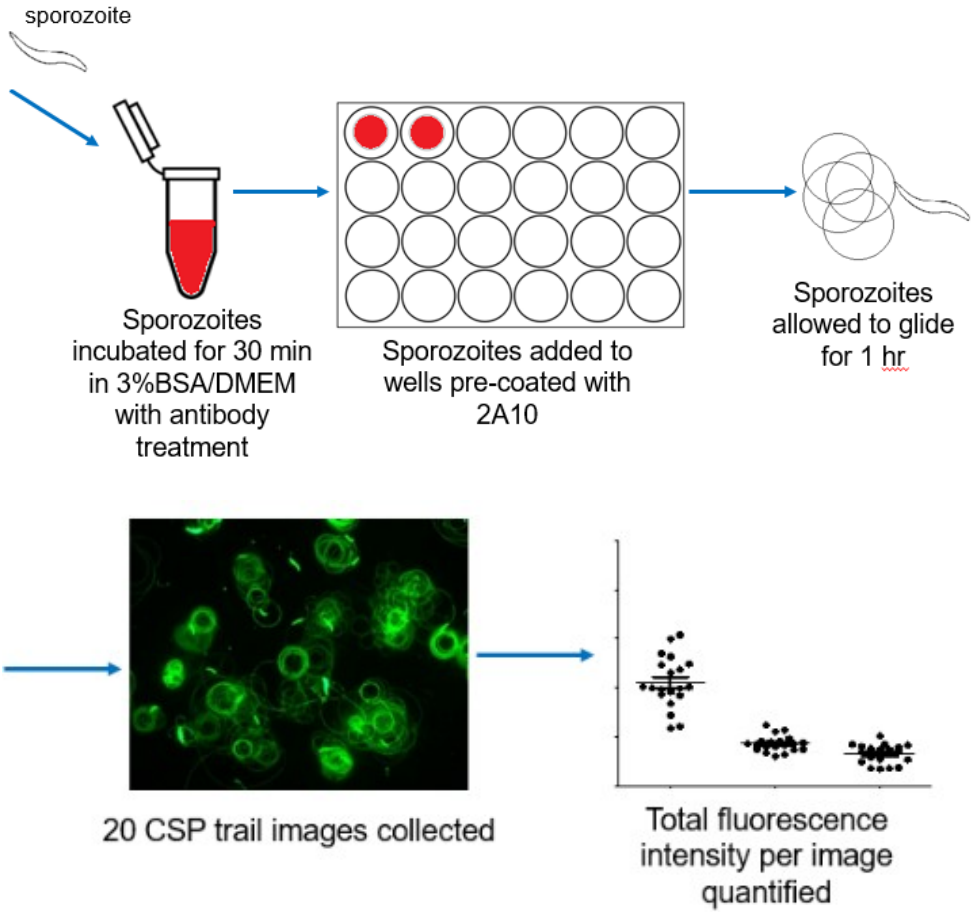

Figure 3. Schematic of the fluorescence intensity assay. Pictorial representation of method used to quantify CSP trails. *P. falciparum* sporozoites were isolated and incubated in 3%BSA/DMEM for 30 min at 25°C. Sporozoites were added to wells pre-coated with 2A10 and allowed to glide for 1 hr at 37°C in 5% CO2 incubator. After fixation and staining, sporozoites were imaged and fluorescence intensity was quantified using the program NIS Elements.

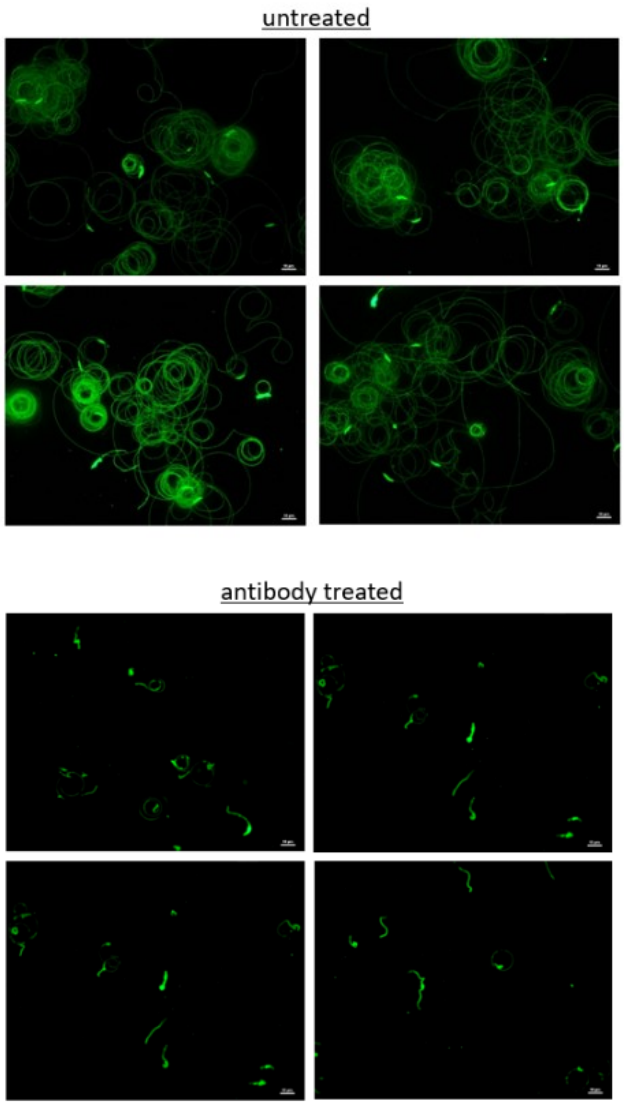

Figure 4. Examples of gliding motility images collected. Images of gliding motility showing the range of trails observed in untreated versus antibody treated sporozoites. Sporozoites were treated with 10ug/mL 2A10. Trails are stained green. Scale bar is 10µm.

A)

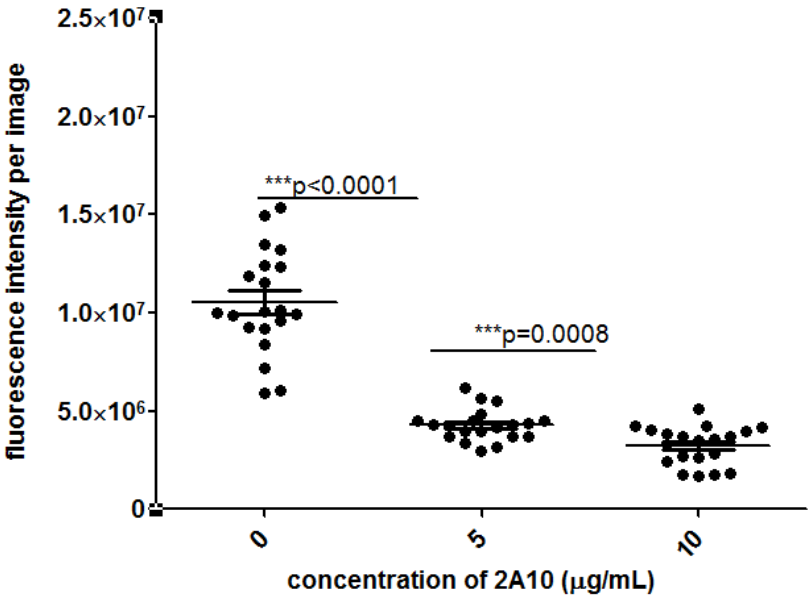

B)

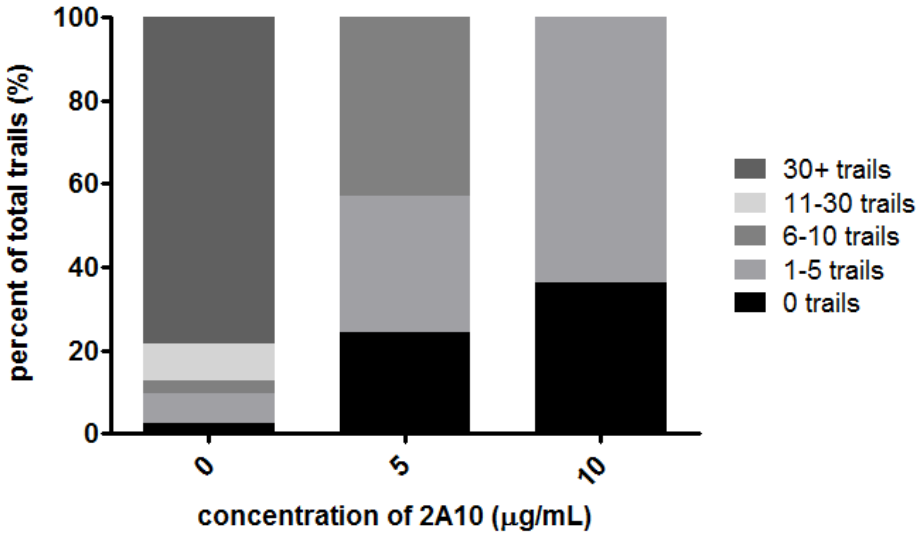

Figure 5. Comparison of the classic trail gliding assay to the fluorescence intensity assay. (A) Sporozoites were treated with the indicated of mAb 2A10 and then added to wells. Sporozoites were allowed to glide for 1 hr after which CSP trails were stained, 20 images were acquired, and their fluorescence intensity quantified. Each dot represents total fluorescence intensity of 1 image. (B) The same wells were quantified using the classic trail gliding assay method of counting sporozoites associated with trails.

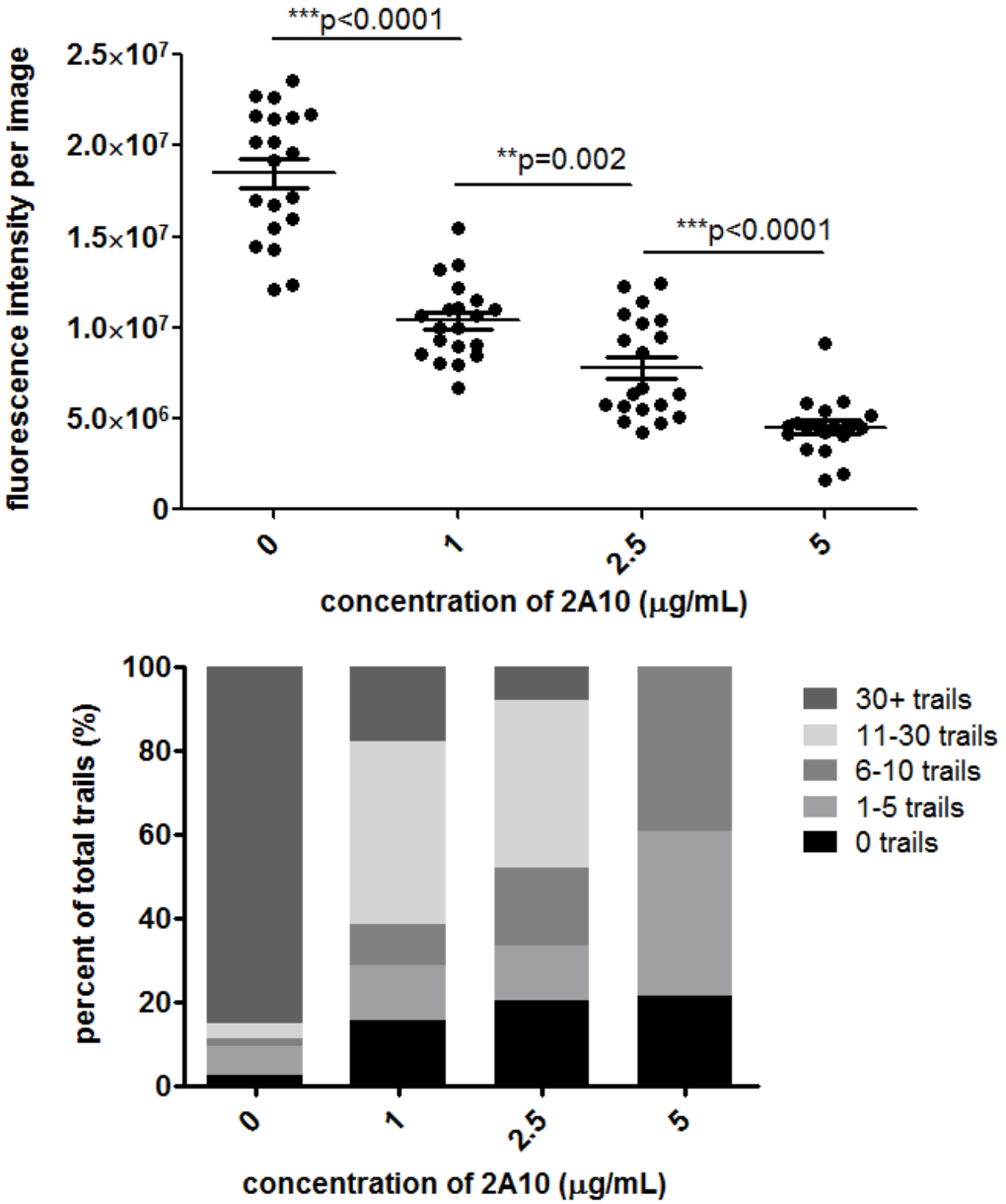

Figure 6. Comparison between the fluorescence intensity assay and classic gliding motility assay with lower concentrations of inhibitory antibody.

A)

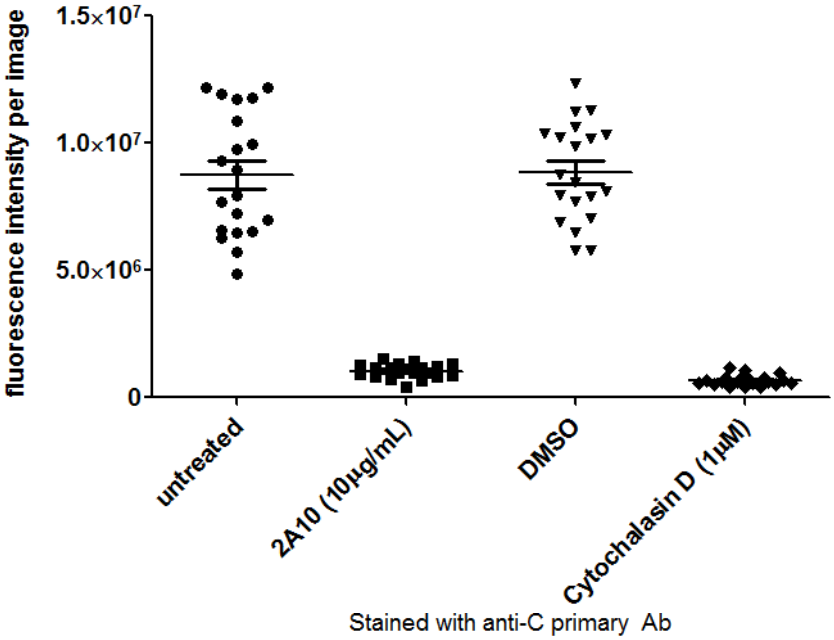

B)

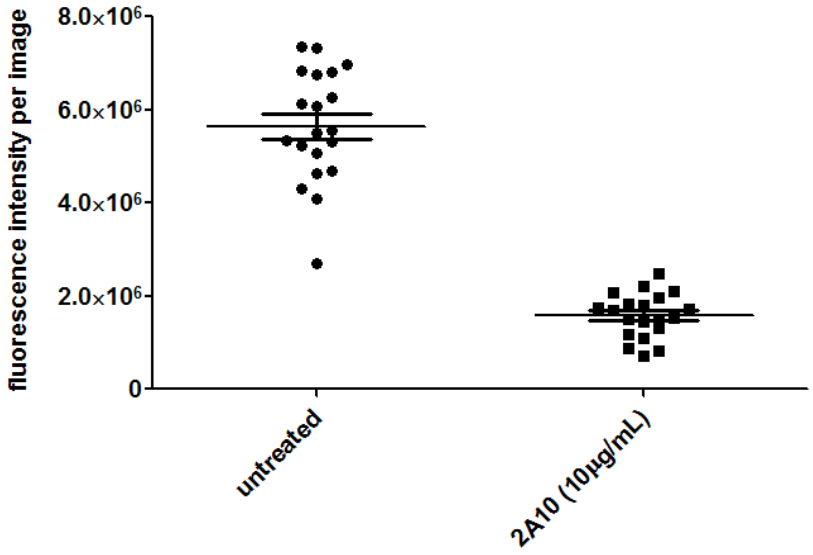

Figure 7. Verification of fluorescence intensity assay using another inhibitor and a different detection antibody. (A) Sporozoites were treated with 1 µM cytochalasin D to inhibit gliding and then stained as normal. (B) Sporozoites were stained with a detection antibody against the C terminus of CSP to verify that inhibition of gliding was not due to competition between inhibitory 2A10 and biotinylated 2A10

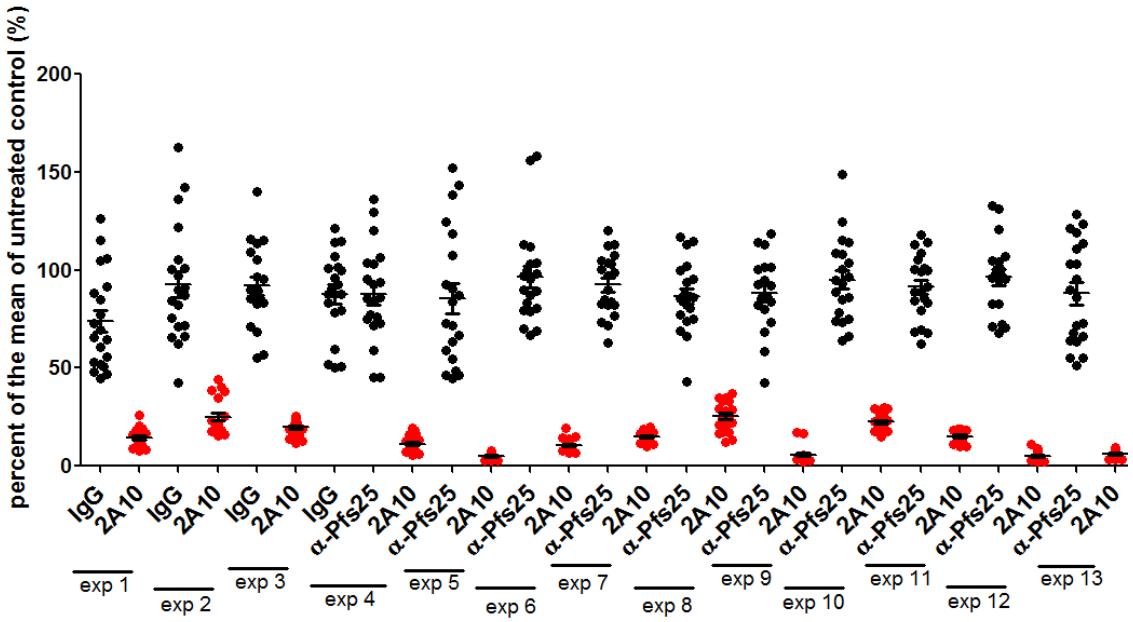

Figure 8. Reproducibility of fluorescence intensity assay. Sporozoites were pre-treated with 2A10 or a control antibody. The fluorescence intensity of the treated wells was normalized to the mean of its relative untreated control. The concentration of 2A10 was 10 µg/mL and the concentrations of human IgG and α-Pfs 25 were 50 µg/mL. Data are from 13 separate experiments.

Testing of the PATH MVI human monoclonal antibodies

Since the fluorescence intensity assay allows for much faster quantification of gliding motility, we decided to scale up the assay to medium throughput by using all 24 wells in a 24 well plate. This allowed for 3 controls and a maximum of 21 monoclonals to be tested per experiment. For ease of comparison of all the monoclonals between experiments, the data of each monoclonal has been normalized to the mean of α-Pfs 25 of its relative experiment. Each monoclonal was tested at a concentration of 50 μg/mL. Testing of mAbs targeting 11 different antigens was performed. The antigens are blinded but their HEPA numbers are given below.

HEPA 103 and HEPA 106

20 HEPA 103 and 21 HEPA 106 monoclonal antibodies were tested (Fig. 9A and B). None of the monoclonals showed marked inhibition and therefore were not selected for further testing.

HEPA 112 and HEPA 113

22 HEPA 112 and 12 HEPA 113 monoclonals were tested (Fig. 10A and B). mAbs 1804, 1787, and 1803 showed some inhibition but none were selected by PATH for additional testing.

HEPA 120 and HEPA 126

9 HEPA 120 and 13 HEPA 126 monoclonals were tested (Fig. 11A and B). None of the monoclonals showed marked inhibition of gliding and therefore were not selected for further testing.

HEPA 121 and HEPA 124

11 HEPA 121 and 18 HEPA 124 mAbs were tested (Fig. 12A and B). From the HEPA 121 monoclonals, mAbs 1950, 1955, 1937, and 1948 were selected for repeated testing (Fig. 12A). 1950 and 1948 seemed to show approximately 50% inhibition of gliding upon initial testing but this inhibitory effect seemed to disappear when the experiments were repeated (Fig. 12A). A similar effect was seen when mAbs 2318 and 2325 from HEPA 124 were tested (Fig. 12B). Ultimately, none of the monoclonals from HEPA 121 and 124 showed consistent inhibition and were not selected by PATH for testing in mouse models.

HEPA 109 and HEPA 122

11 HEPA 109 and 15 HEPA 122 mAbs were tested (Fig. 13A and B). From HEPA 109, mAbs 2382, 2394, 2402, 2373, and 2361 were tested more than once (Fig. 13A). mAb 2373 was selected by PATH for progressing to the next experimental phase of testing since at least 40-45% inhibition was observed in 3 separate experiments (Fig. 13A). Apart from 2240 and 2224, all of the mAbs in HEPA 122 were tested more than once (Fig. 13B). Although 2211 was tested 4 times and showed 40-75% inhibition, PATH did not select it for additional experiments (Fig. 13B).

HEPA 125

Out of 21 HEPA 125 mAbs, 13 were tested more than once (Fig. 14). Several mAbs (2153, 2171, 2156, 2169) showed a pattern of being markedly inhibitory upon initial testing but less so when additional experiments were performed (Fig. 14). 2175, 2176, 2178, and 2162 were selected by PATH for testing in mouse models since they consistently showed 50% or more inhibition over 3 separate experiments.

A)

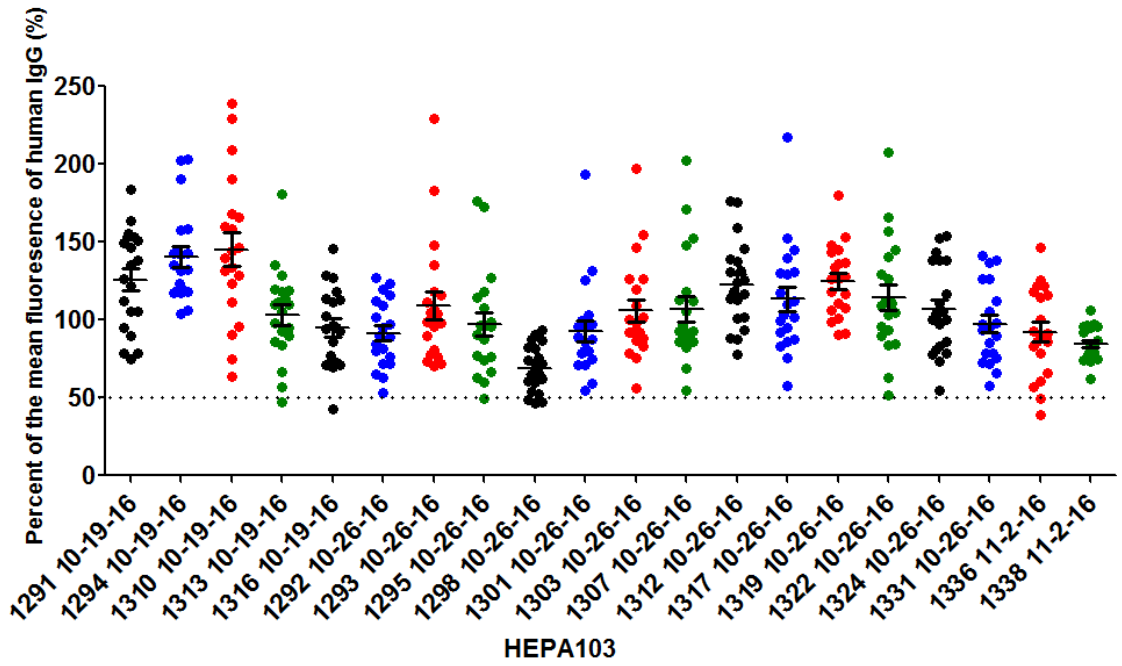

B)

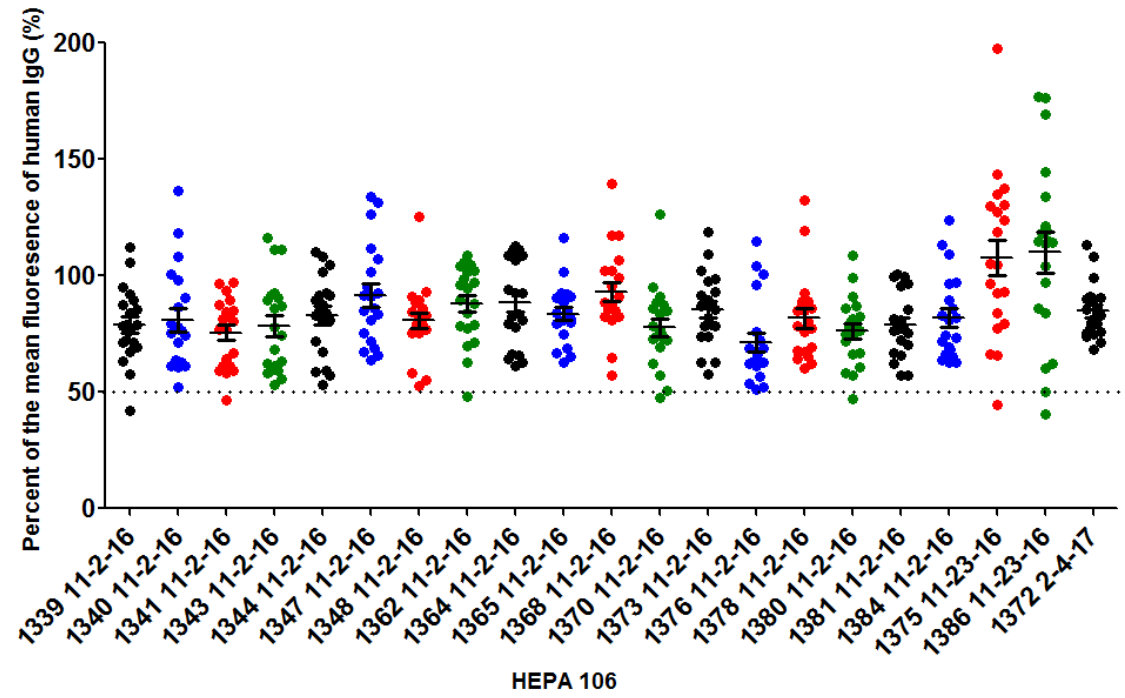

Figure 9.Fluorescence intensity of HEPA103 and HEPA 106 normalized to the mean fluorescence intensity of human IgG. A) HEPA 103. B) HEPA 106.

A)

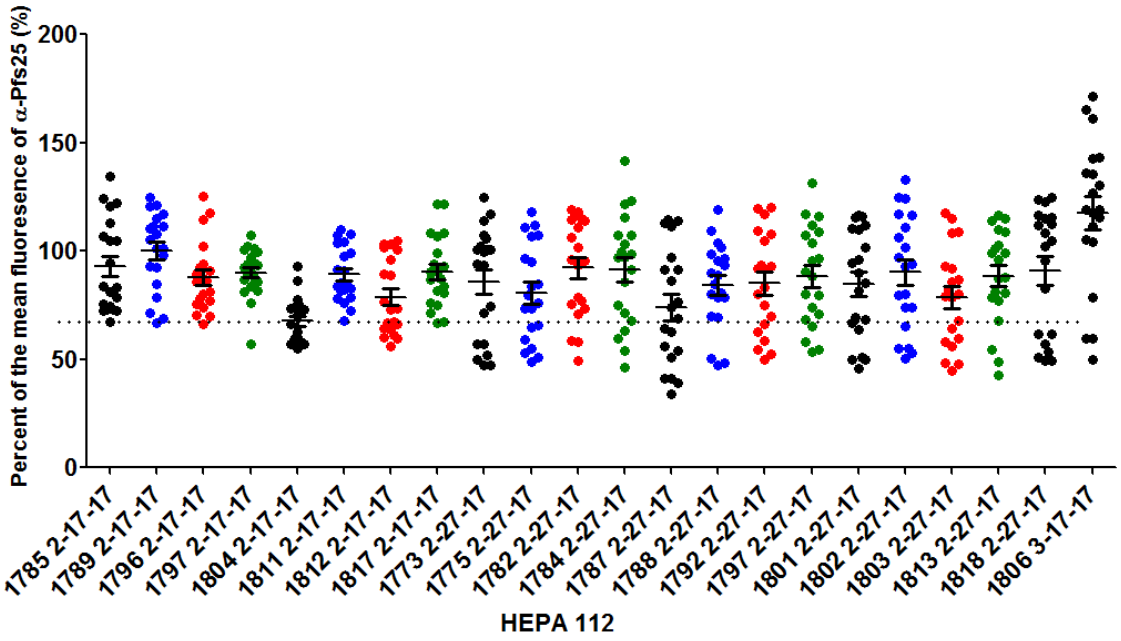

B)

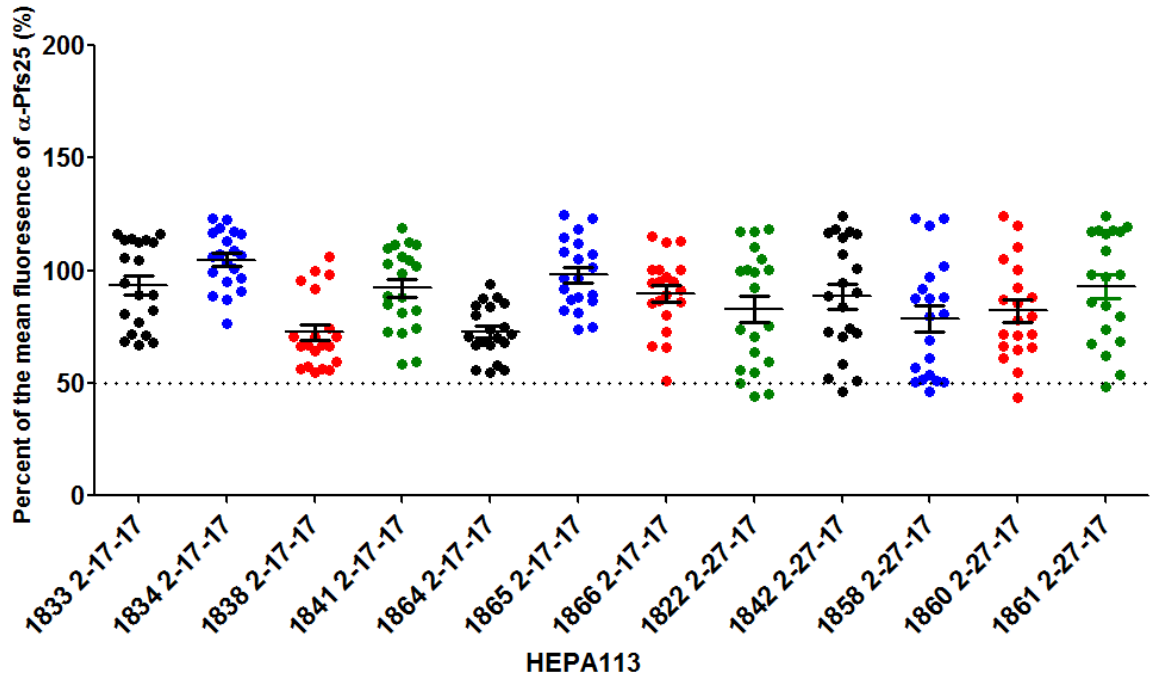

Figure 10.Fluorescence intensity of HEPA112 and HEPA 113 normalized to the mean fluorescence intensity of α-Pfs 25. A) HEPA 112. B) HEPA 113.

A)

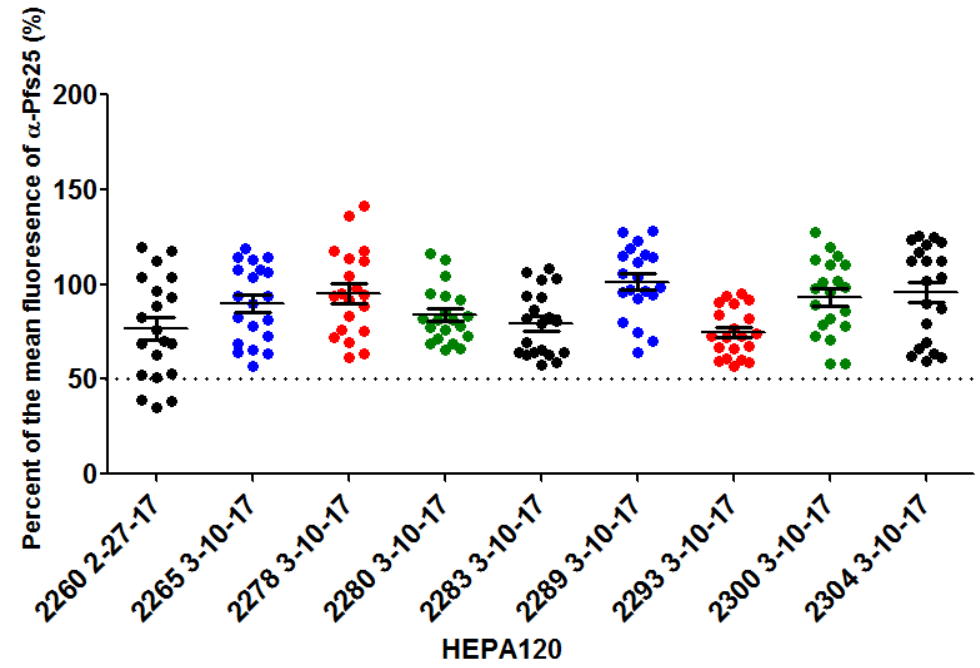

B)

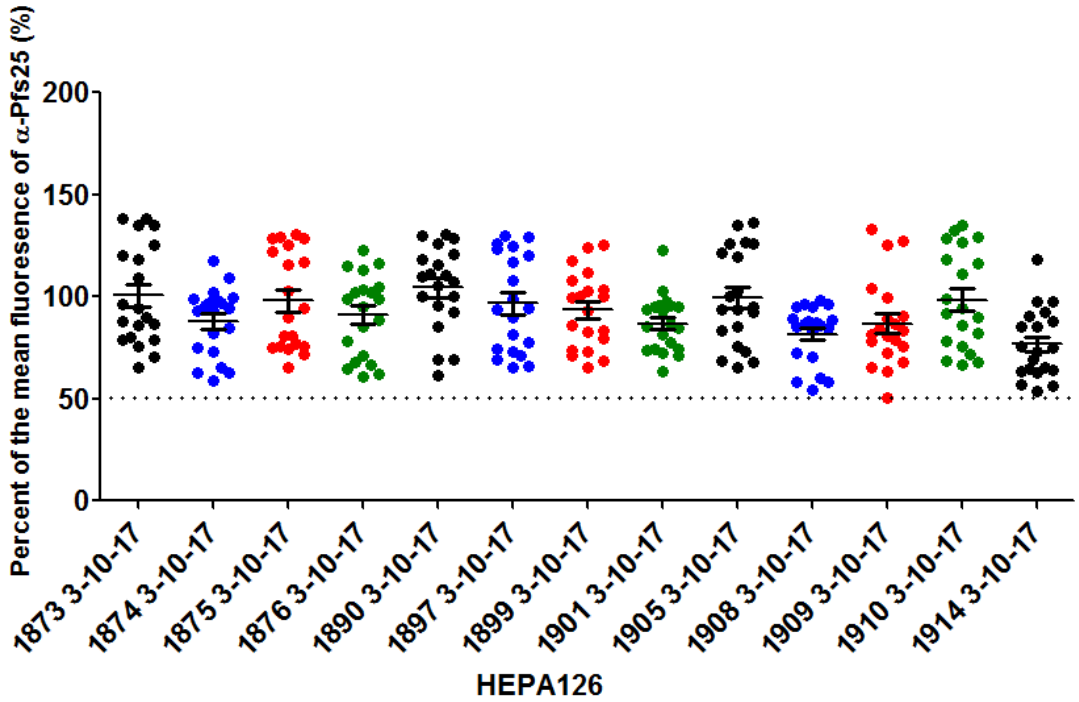

Figure 11.Fluorescence intensity of HEPA120 and HEPA 126 normalized to the mean fluorescence intensity of α-Pfs 25. A) HEPA 120. B) HEPA 126.

A)

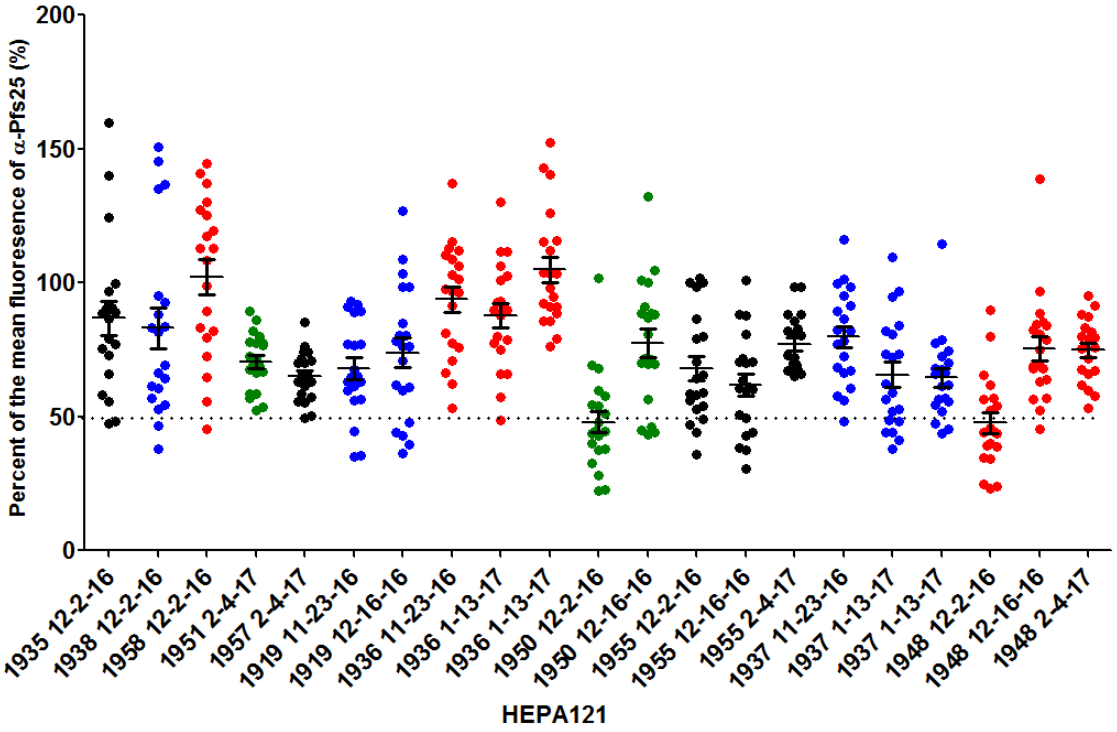

B)

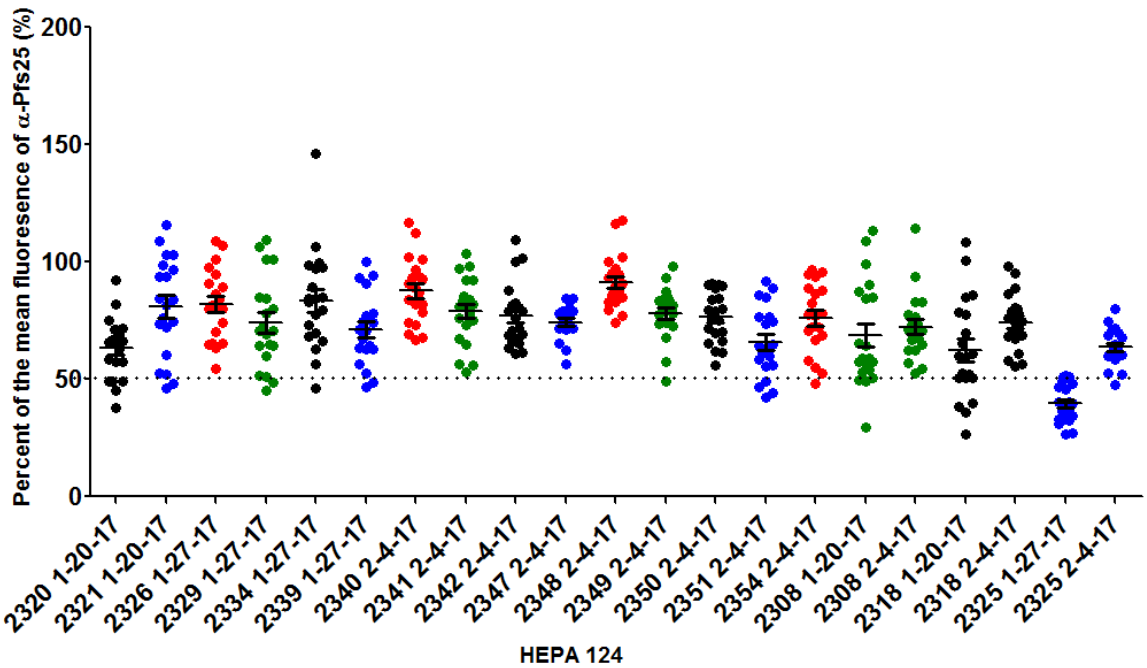

Figure 12.Fluorescence intensity of HEPA121 and HEPA 124 normalized to the mean fluorescence intensity of α-Pfs 25. A) HEPA 121. B) HEPA 124.

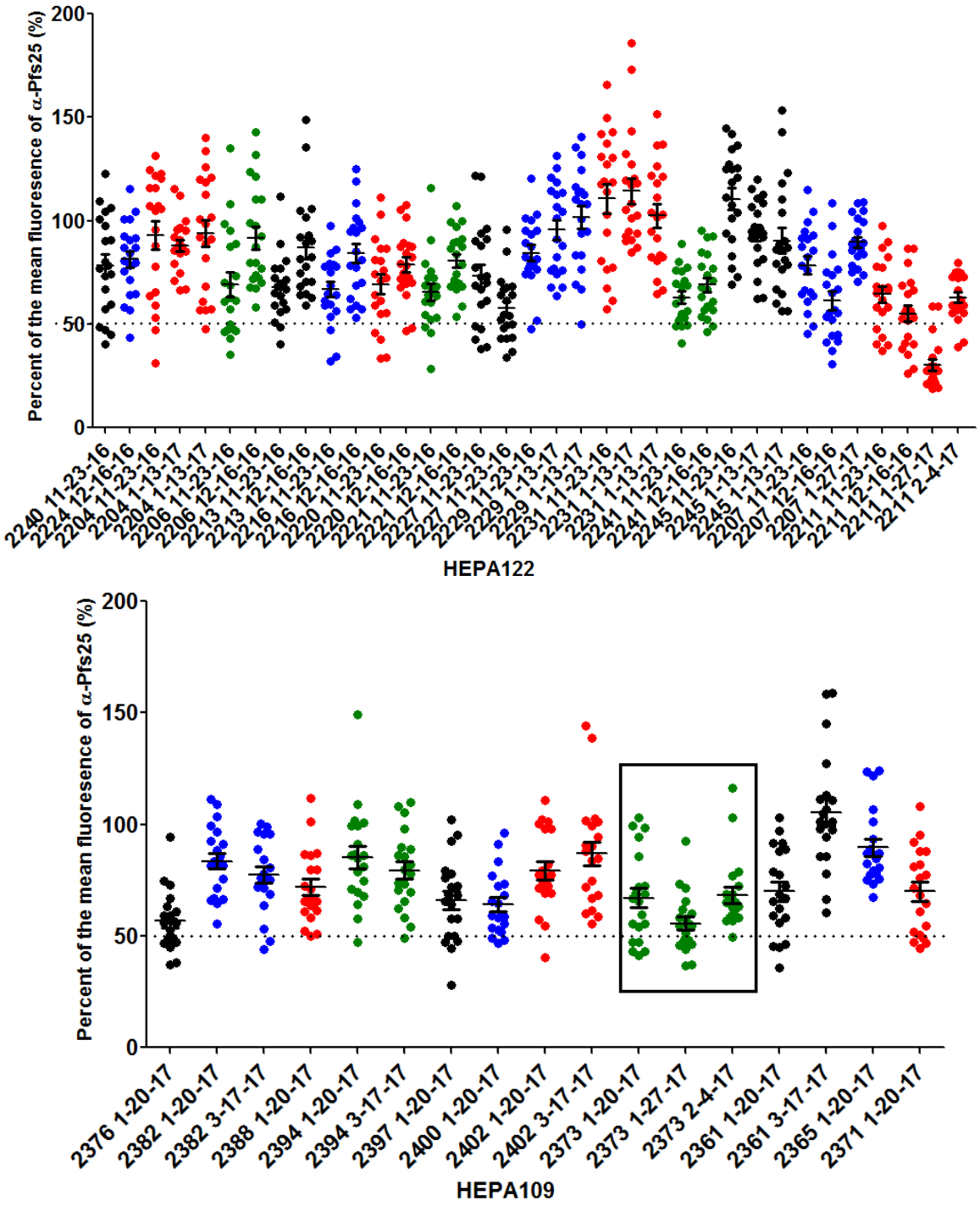

Figure 13. Fluorescence intensity of HEPA122 and HEPA 109 normalized to the mean fluorescence intensity of α-Pfs 25. HEPA 109. mAb 2373 was selected by PATH MVI for the next phase of testing and is shown in the black box.

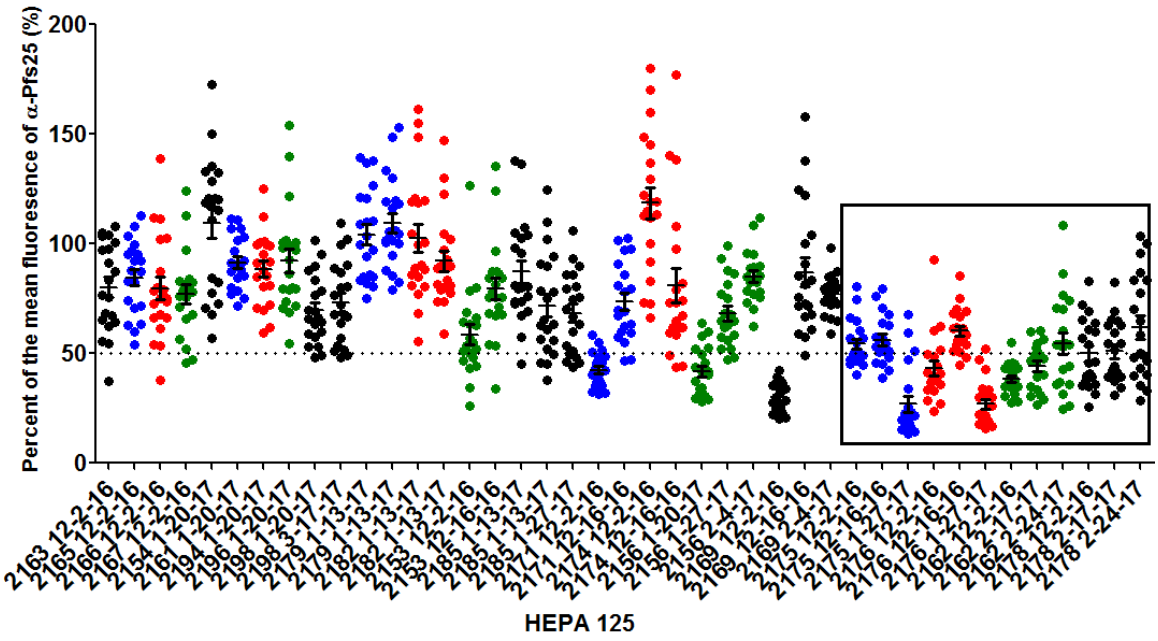

Figure 14.Fluorescence intensity of HEPA 125 normalized to the mean fluorescence intensity of α-Pfs 25. mAbs 2175, 2176, 2162, and 2178 were selected by PATH MVI for the next phase of testing and are shown in the black box.

DISCUSSION

A new method for quantifying gliding motility has been described here and based on experimental data, the fluorescence intensity assay seems to be a useful in vitro method of assessing antibody based vaccines. We believe that our assay can be used to accurately assess antibody mediated inhibition of gliding motility. Our method of quantifying fluorescence intensity of CSP trails has been shown to be both sensitive to very low concentrations of inhibitor and replicable. Statistical analyses is also much easier due to the nature of the fluorescence intensity data. We have also addressed the possibility that the 2A10 primary antibody was interfering with detection of trails; our data shows inhibition of inhibition of gliding motility both with another inhibitor (cytochalasin D) and with another primary antibody (anti-C). Another potential verification of the fluorescence intensity assay is that additional experiments can be carried out with a mutant TRAP-Val parasite that displays impaired gliding. We would expect to see decreased fluorescence intensity in the mutant compared to wild type sporozoites.

Monoclonal antibodies 2373, 2175, 2176, 2162, and 2178 were selected by PATH MVI for further testing. Future experiments for the project will involve the 5 antibodies being tested in mice with humanized livers and observing if passive administration of the mAbs are able to convey some form of immunity against *P.falciparum* in mice. 4 out of the 5 mAbs deemed to show at least 50% inhibition of gliding come from HEPA 125; this suggests that the HEPA 125 antigen might be a potential vaccine target. In order to confirm that the inhibition seen in the 5 mAbs is due solely to the antibodies binding to the *P. falciparum* sporozoites and inhibiting their gliding, an additional control could be carried

out where the mAbs are tested with *P. berghei* sporozoites. Ideally, we would not see the same levels of inhibition as the mAbs would not bind to the parasites. Our data suggests that the majority of the 188 mAbs we tested do not inhibit gliding motility consistently.

An interesting trend seen several times when testing monoclonals from HEPA 125, 121, 124, and 109 was that the first test showed marked inhibition of gliding motility but subsequent tests did not. A potential reason for this could be that antibodies were freshly thawed before the first test and then left at 4 in the fridge for subsequent experiments. Perhaps the concentration of the antibodies changed while in the fridge due to sticking to the tube or lost the ability to bind to sporozoites as efficiently. This could explain why freshly thawed antibodies were more potent inhibitors of gliding. Another reason for this could be batch to batch variation of sporozoite motility.

Due to project time constraints many antibodies were only tested once and based on initial data, antibodies were selected for repeated testing. PATH also directed us to repeat certain mAbs based on data from the other in vitro tests that were being carried out in other labs. This could be seen as biasing the results toward mAb candidates that were suspected to be inhibitory. Ideally, we would like to test all the antibodies 3 times to be certain that natural variation in gliding or the freshly thawed antibody hypothesis described above did not demonstrably influence the data.

TRAP STAINING OF NON-GLIDING AND GLIDING SPOROZOITES

INTRODUCTION

CSP uniformly coats the surface of the sporozoite and has multiple functions throughout the pre-erythrocytic stage of malaria [19]. The structure of CSP consists of an N terminal domain containing a proteolytic cleavage site [19], a repeat region, and a TSR domain in the C terminal region (Fig. 15B). A KLKQP sequence is found at the start of the repeat region and is highly conserved among all *Plasmodium* species (Fig. 15A) [10, 14]. The TSR domain consists of a 60 molecule long region that has cell adhesion properties (Fig. 15B) [19]. The repeat region of CSP in *P. berghei* consists of 3 distinct repeated sequences NPNDPPP, NANDPPP, and PQPQ (Fig. 15A). Studies have shown that CSP plays a vital role in sporozoite infectivity of salivary glands and sporozoite development [8, 13, 21]. However, the precise role of the repeat region is still being studied. The complete deletion of the repeat region or the repeat region and N terminal has been shown to lead to impaired sporozoite development but there was no effect on oocyst formation [13]. The ΔRep mutant produced sporozoites but they were unable to mature and the ΔNΔRep mutant was unable to produce any sporozoites [13]. This suggests that the repeat region is vital for sporozoite development perhaps playing a structural role or affecting other sporozoite membrane proteins [13].

In order to explore the more subtle phenotypes of the repeat region, our lab generated 5 mutant parasite lines (Fig. 15B). In ΔRep1, ΔRep2, and ΔRep3 their respective repeat region was deleted. ΔDtoN had the aspartic acid residues switched to asparagine in order to change the charge of the residues but maintain structure. ΔScr had the repeats randomly

scrambled throughout the repeat region. An RCon (not shown) mutant was also generated in order to control for transfection.

Our lab conducted paired live gliding assays in order to compare mutant motility to wild type controls (Fig. 16A and B, unpublished data [5]). In the rodent model used, the majority of WT sporozoites were shown to glide in a circular fashion and this was also seen in ΔRep1 and ΔRep3 (Fig. 16A), suggesting that the first and third repeat regions might not play as important of a role in motility. This was corroborated by measuring the median speed of sporozoites in live gliding assays (Fig. 16B). WT, ΔRep1, and ΔRep3 sporozoites glide at a median speed of approximately 1.5μm/sec suggesting that the mutants are gliding in the same manner as WT. However, ΔRep2 and ΔScr sporozoites mostly displayed a disrupted waving or patch gliding motility (Fig. 16A). This suggests that the second repeat region is required for normal gliding motility and scrambling the repeats results in the loss of normal motility as well. ΔRep2 and ΔScr have a significantly lower median speed (Fig. 16B), supporting the hypothesis that patch and wave gliding are irregular and that these two mutants have a disrupted motility. ΔDtoN seems to show a subtler, intermediate phenotype where sporozoites show slightly greater levels of patch and wave gliding than the more severely affected mutants but the majority of parasites still glide in a circular manner (Fig. 16A). The median speed of ΔDtoN sporozoites is significantly lower than WT but not as low as ΔRep2 and ΔScr suggesting that ΔDtoN is not as efficient at circular gliding as WT but still capable of doing so (Fig. 16B).

Our lab has also investigated the adhesion site turnover of our mutant parasites in order to investigate how mutating CSP affects sporozoite ability to attach to an extracellular

substrate and how greatly adhesion site turnover affects motility (Fig. 17A and B, unpublished data). Using reflection interference contrast microscopy (RICM), we observed that WT, ΔRep1, and ΔRep3 sporozoites show a similar turnover rate of 22-32 adhesion sites/2.5 min (Fig. 17B). However, ΔDtoN, ΔRep2, and ΔScr show significantly lower turnover rates with ΔRep2 and ΔScr showing more severe phenotypes (Fig. 17B). The lack of adhesion site turnover supports the previously median motility speed data that showed that ΔRep2 and ΔScr moved much slower than WT.

Since adhesion sites were shown to be affected by CSP mutation, we wanted to explore how TRAP is distributed on the surface of our mutants. Thrombospondin-related anonymous protein (TRAP) is a type I transmembrane protein found in the micronemes of the sporozoite [19]. Its extracellular domain consists of two adhesion domains: an A domain and a TSR [11]. It has been suggested that TRAP connects the actomyosin motor complex of the sporozoite to extracellular proteins [21] and sporozoite motility depends on TRAP adhesion turnover [11]. When the parasite takes part in gliding motility, the sporozoite moves forwards and TRAP and the intracellular motor moves backwards [11]. Using this model and previous studies, we believe the movement of TRAP from the posterior end of the sporozoite is necessary for gliding motility [11]. When TRAP is deleted, sporozoites are unable to move [11]. It is been shown a rhomboid protease is required to cleave TRAP in order for it to be shed and if the rhomboid-cleavage site is mutated, not only is TRAP not shed but gliding motility and infectivity as reduced [11, 26]. These are phenotypes are similar to what we have observed in our CSP mutant parasites. However, currently there is no known interaction between CSP and TRAP and it is unclear

how mutations in the repeat regions would impact TRAP shedding. In order to investigate the link between CSP and TRAP adhesive interactions, here we demonstrate the TRAP staining patterns of WT and CSP mutant sporozoites in non-gliding and gliding conditions.

A)

KLKQP PPPP NPNDPPPP NPNDPPPP NPNDPPPP NPNPPPPP NANDPPPP NANDPAPP NANDPAPP NANDPAPP NANDPAPP NANDPAPP NANDPAPP NANDPPPP NPNDPAPP QGNNN PQPQ PRPQ PQPQ PQPQ PQPQ PQPQ PRPQ PQPQP

B)

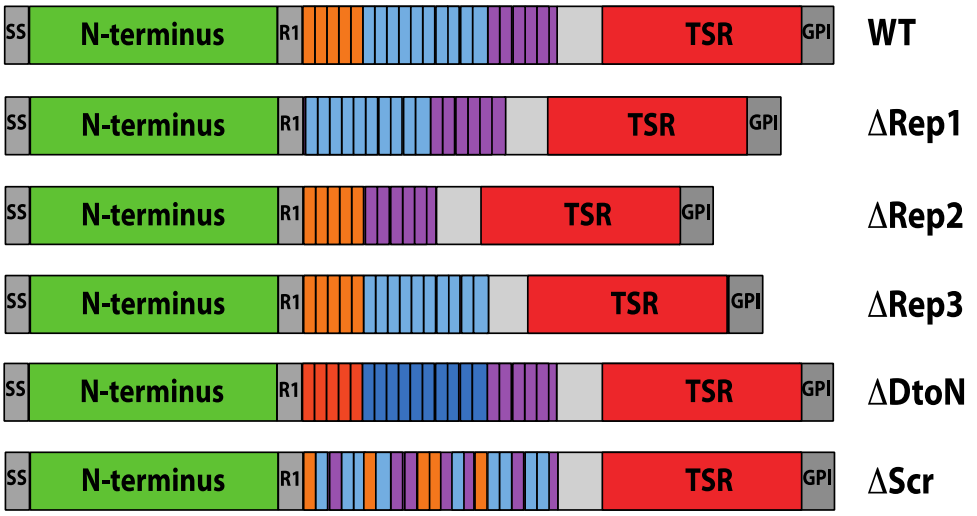

Figure 15. Schematic representations of CSP and the CSP repeat amino acid sequence. A) The amino acid sequence of the *P. berghei* CSP repeats showing the KLKQP sequence and the 3 repeat regions. B) Schematic comparisons of WT CSP to our mutant parasites. ΔRep1, ΔRep2, and ΔRep3 have their respective repeat region deleted. ΔDtoN has the aspartic acid residues switched to asparagine. ΔScr has its repeats randomly scrambled.

A)

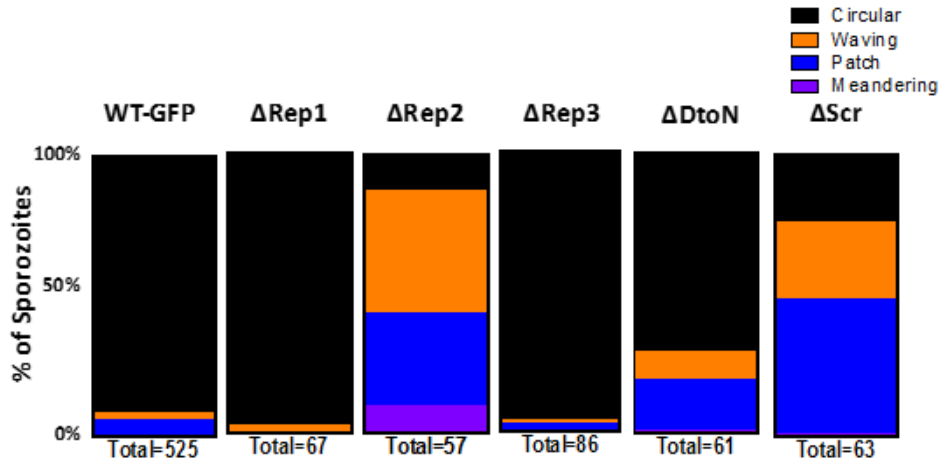

B)

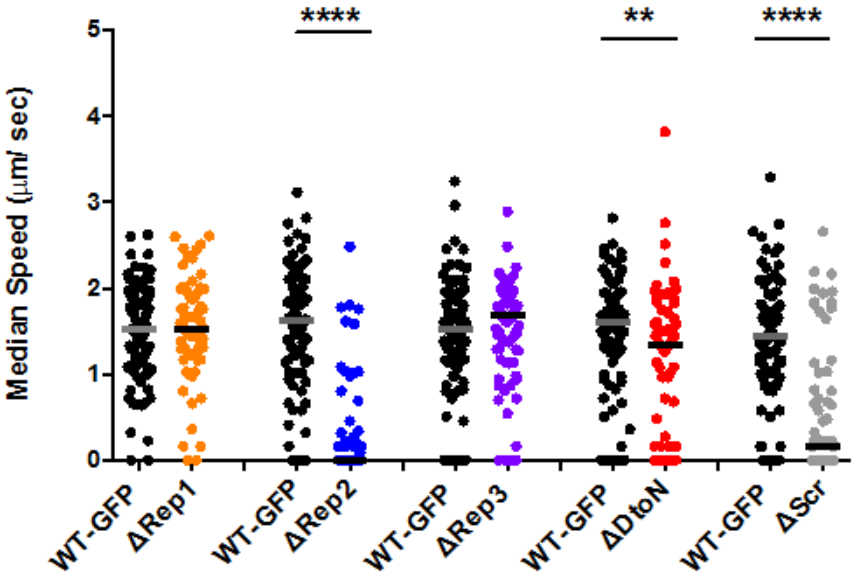

Figure 16. Categorization of motility and median speed seen in wild type and mutant parasites in live gliding assays [5, unpublished data]. A) Paired live gliding assays were carried out with wild type and mutant sporozoites and 4 categories of motility were observed. B) The median speed of the same gliding parasites was obtained.

A)

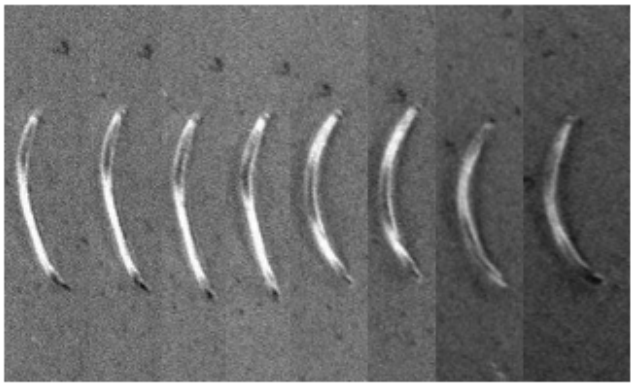

B)

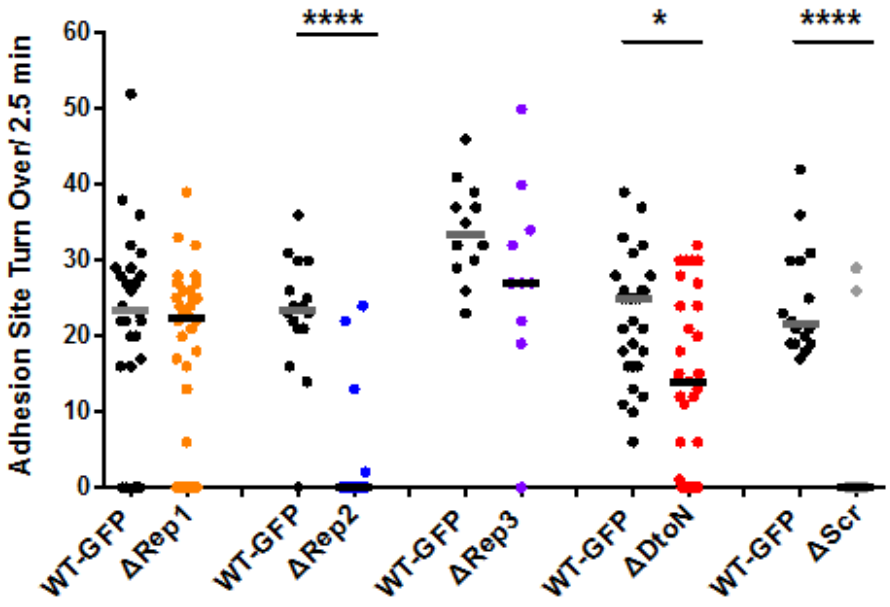

Figure 17. Turnover of adhesion sites in wild type and mutant parasites as analyzed by RICM [5, unpublished data]. A) Visualization of adhesion site turnover over time. Adhesion sites are shown as dark patches. B) Differences in adhesion site turnover between wild type and mutant sporozoites.

METHODS

Generation of mutant parasites and parasite transfection

Mutant parasites were generated as described previously [13]. For each of the mutants the endogenous csp gene was replaced with a csp gene in which the repeat sequence of CSP was truncated, the repeats were scrambled, or the charge of residues reversed by converting aspartate to asparagine. Parasites were transfected as described previously [13].

Parasite development in Anopheles stephensi

Parasites were allowed to develop in the mosquito following a blood meal as described previously [13]. Between day 21 and 22 post blood meal, salivary glands were collected and sporozoites were isolated.

Immunofluorescence assays

Glass coverslips were placed in two 24 well plates, one for gliding and one for non-gliding. Mosquitoes were dissected in L-15 (Leibowitz 15) and salivary glands were obtained. The salivary glands were pelleted by spinning down for 6 seconds. The media was removed and replaced with 200 μL of fresh, cold L-15. The sporozoites were then isolated and counted. 400 μL containing 10000-50000 sporozoites in L-15 was then added to each well. The sporozoites were spun for 4 minutes at 300g with an acceleration of 3 minutes and no brake deceleration.

The media was removed from the non-gliding wells and the sporozoites were fixed with cold 4% paraformaldehyde for 1 hour at room temperature. After the removal of the media from the gliding wells, 400 µL of 2% BSA/L-15 pH 7.4 was added per well. The gliding plate was placed in a 5% CO2 incubator for 1 hour to allow sporozoites to glide. After gliding, the sporozoites were fixed as per the non-gliding well.

After fixing, the wells were washed 3 times with 1x PBS pH 7.4. The wells were blocked with 1%BSA/5% goat serum/BSA for 1 hour at 37°C. The wells were then stained with primary antibody for 1 hour at 37°C, washed 3 times with PBS, and then stained with secondary antibody for 1 hour at 37°C. The primary antibodies used were either polyclonal α-TRAP (1:100 dilution) or IgG purified α-TRAP (1:100 dilution). The secondary used was a goat anti-rabbit (H+L) highly cross adsorbed antibody conjugated to Alexa fluor 594 [A-11037]. After staining, the wells were washed 3 times with PBS. The coverslips were carefully removed from the wells, allowed to dry for 10 minutes, and then mounted to slides with ProLong Gold antifade DAPI mounting media overnight. The coverslips were then sealed with clear nail polish and imaged using the 100x oil objective of a fluorescent microscope. Sporozoites were picked using bright field and categorized using the fluorescent channel. Over 100 sporozoites were counted and categorized according to the following: no stain, punctate, patched, and whole stain.

Statistical analyses

To determine significance of results, paired T-tests were carried out with a 95% confidence interval

RESULTS

Four categories of TRAP staining were observed in wild type sporozoites in non-gliding and gliding conditions: unstained, punctate staining, patch staining, and whole staining. (Fig. 18 and Fig. 19). Unstained signified no stain on the sporozoite and punctate staining signified a dotted staining (Fig. 18). Patch staining signified a large patch in either the center of the sporozoite or at the posterior end (Fig. 19). Whole staining signified the entire parasite being fluorescent. There seem to be marked differences in TRAP staining between non gliding and gliding wild type sporozoites (Fig. 20). In non-gliding conditions there was a significantly greater percentage of unstained sporozoites ($p<0.0001$) whereas in gliding conditions, there was a significantly greater percentage of patch stained sporozoites ($p<0.0001$). Gliding sporozoites also seemed to show a significantly greater ($p=0.0091$, $p=0.0231$) percentage of punctate and whole staining (Fig. 20). This data supports the idea that TRAP is shed when sporozoites start to move.

In order to address concerns that 1 hour of gliding might be too long and might lead to sporozoite death, we carried out a side by side comparison of sporozoites glidng for 20 minutes and 1 hour (Fig. 21). This experiment was also carried out using an IgG purified antibody to TRAP in order to minimize background. As observed before the percent of unstained sporozoites in non-gliding conditions is 55% and this number decreases as sporozoites begin to glide and secrete TRAP. A greater percentage of patched sporozoites is seen in the 1 hour gliding condition compared to the 20 minute gliding condition (Fig. 21). Less than 10% of sporozoites are whole stained under all the 3 conditions and the percent of punctate stained sporozoites does not seem to vary between 20 minutes and 1

hour conditions (Fig. 21). Since the percent of punctate and whole stained sporozoites was quite small, for ease of comparison going forward we have grouped punctate, patched, and whole stained sporozoites as just 'stained'.

In order to further investigate TRAP staining, mutant sporozoite IFAs were performed with a WT control (Fig. 22A and B). Non-gliding ΔRep1, ΔRep3, ΔDtoN, and RCon sporozoites show a similar percent stained to that of their non-gliding WT controls where approximately 30-40% of parasites show some form of TRAP stain (Fig. 22A). ΔScr shows the most marked difference from where less than 10% of non-gliding sporozoites show TRAP staining compared to 30% stained in its WT control (Fig. 22A). In gliding conditions, ΔRep1, ΔRep3, and RCon sporozoites show a similar percent stained compared to their WT controls where over 75% of sporozoites show TRAP staining. (Fig. 22B). Gliding ΔDtoN sporozoites seem to show a slightly lower percentage of stained parasites compared to WT (Fig. 22B). ΔScr again shows the greatest deviation from WT with less than 10% of sporozoites showing TRAP staining compared to over 90% in WT (Fig. 22B).

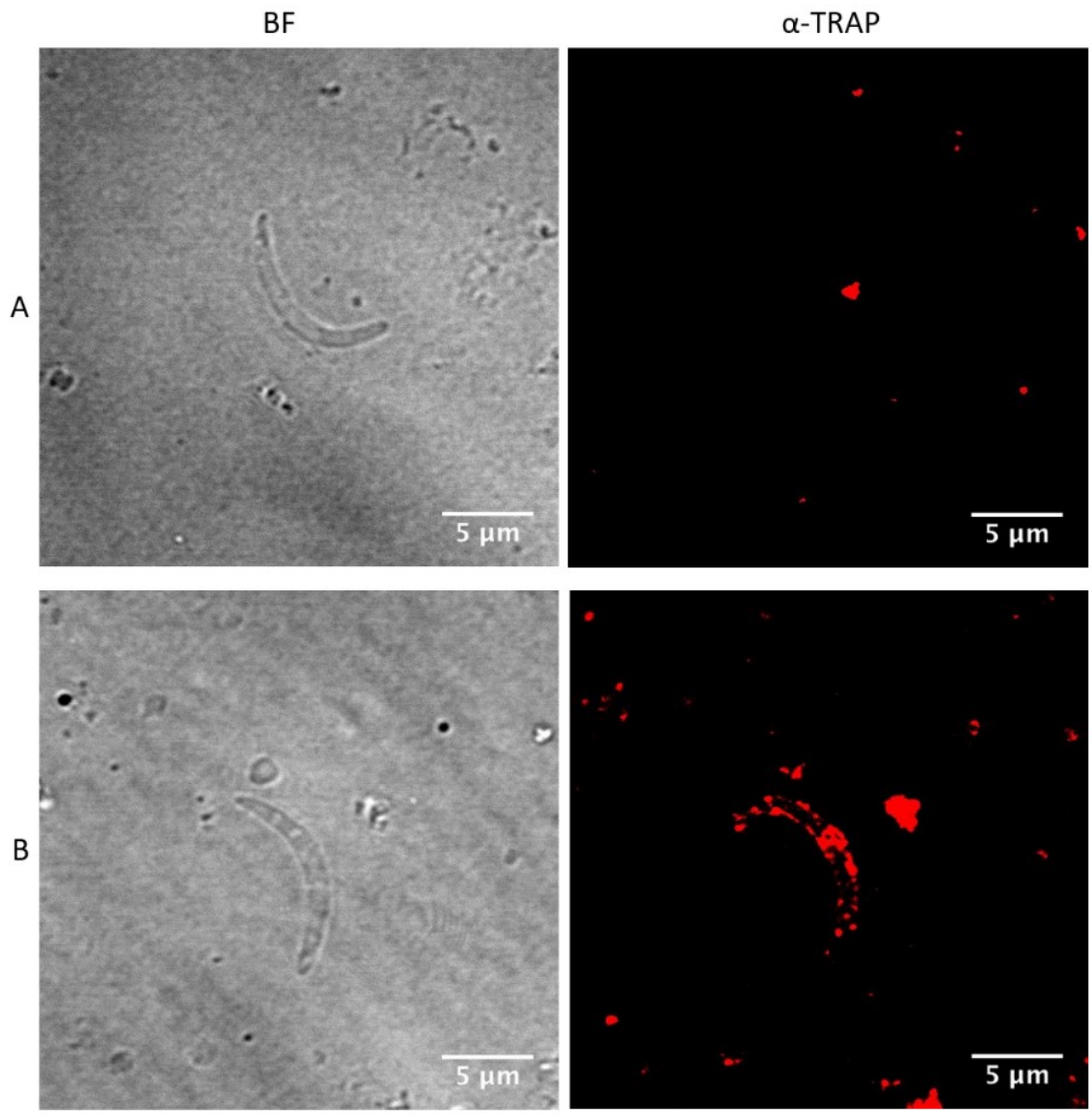

Figure 18. Examples of TRAP staining observed in sporozoites. TRAP is stained red. Scale bar is 5µm. A) Unstained. B) Punctate with a center patch.

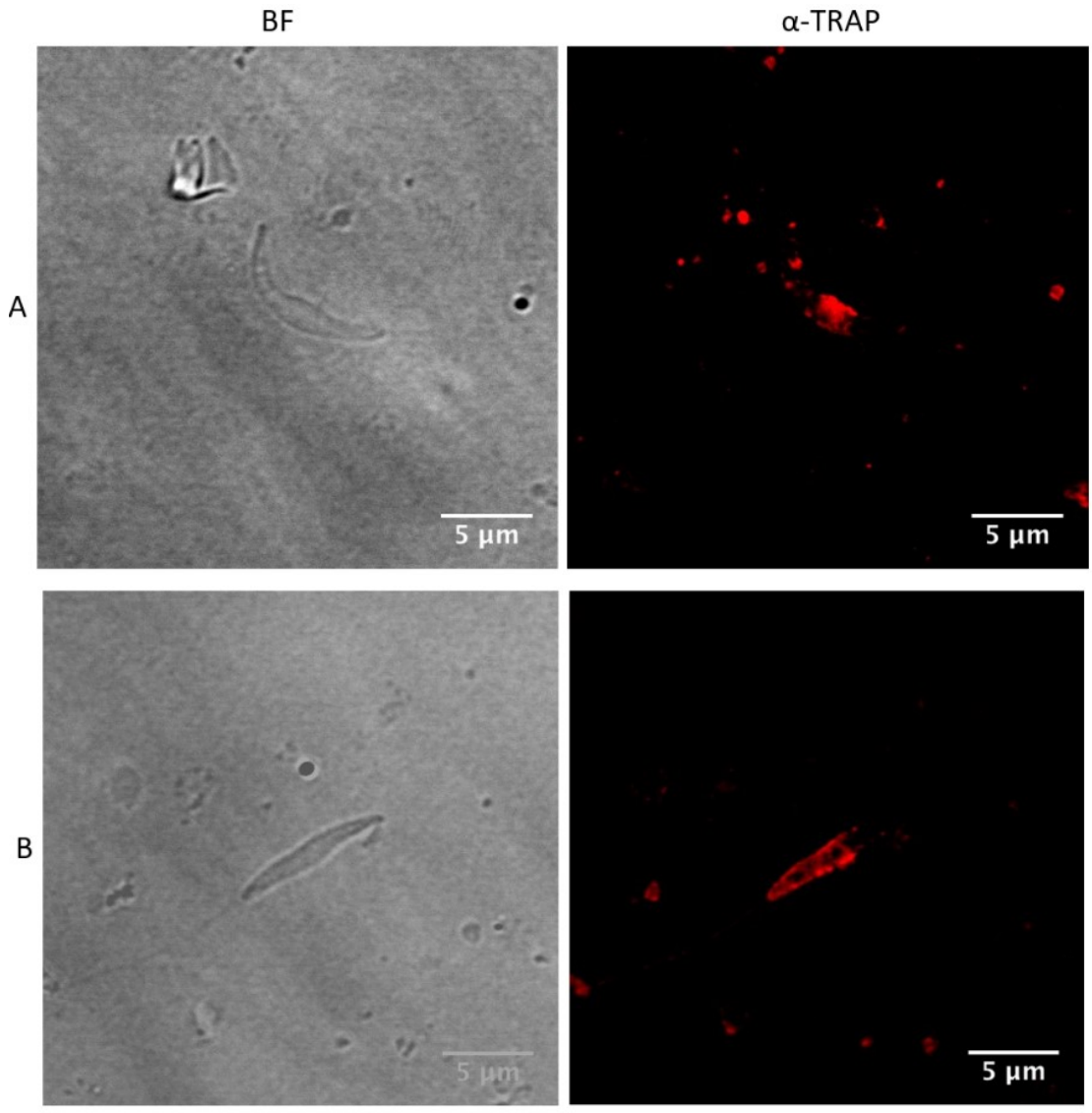

Figure 20. Examples of patched TRAP staining observed in sporozoites. TRAP is stained red. Scale bar is 5µm. A) Central patch staining. B) Posterior patch staining.

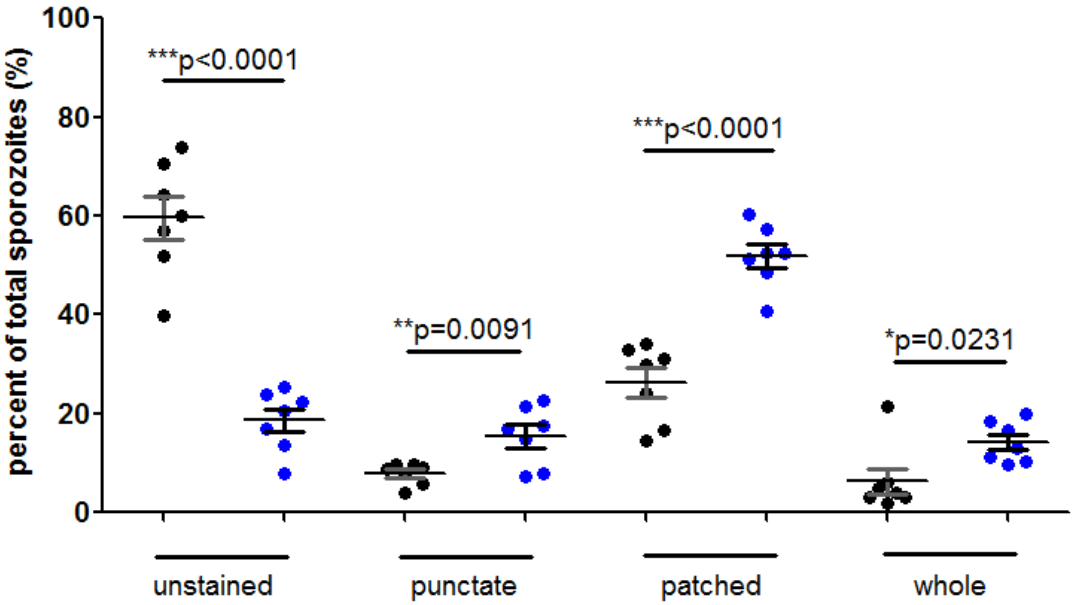

Figure 20. Comparison of wild type sporozoite TRAP staining patterns in non-gliding and gliding conditions. Sporozoites were allowed to glide on glass coverslips for 1 hr after which they were fixed and stained. Coverslips were imaged and TRAP staining patterns of 100 sporozoites were categorized.

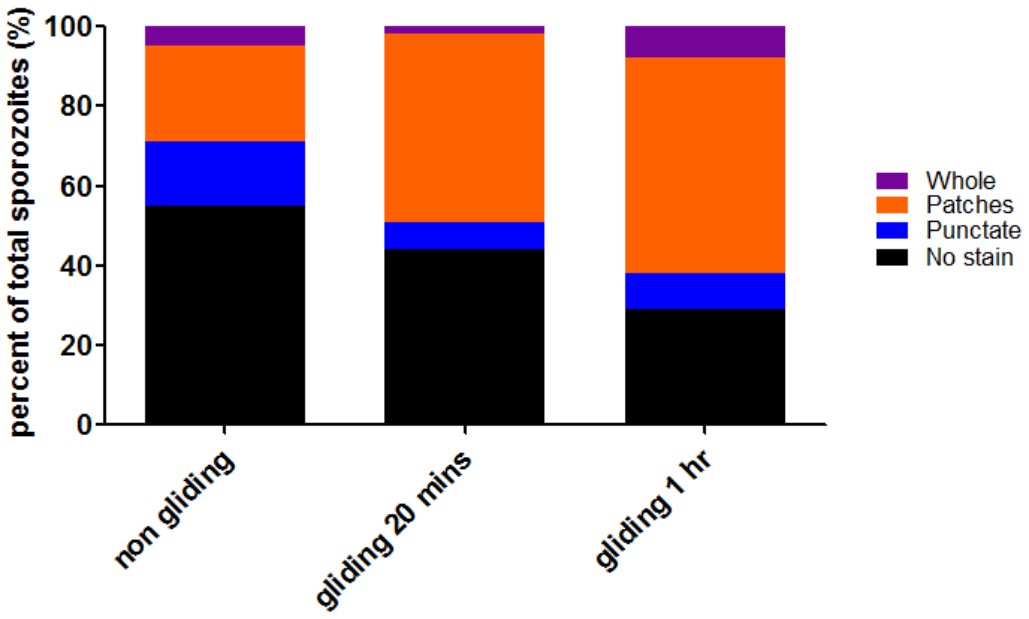

Figure 21. Comparison of TRAP staining patterns in sporozoites gliding for 20 min vs 1 hr. Non gliding sporozoites were instantly fixed with 4% PFA after parasites were spun onto coverslips. Gliding sporozoites were incubated at 37°C for 20 min then fixed. In a separate 24 well plate, sporozoites were allowed to glide for 1 hr at 37°C before fixation.

A)

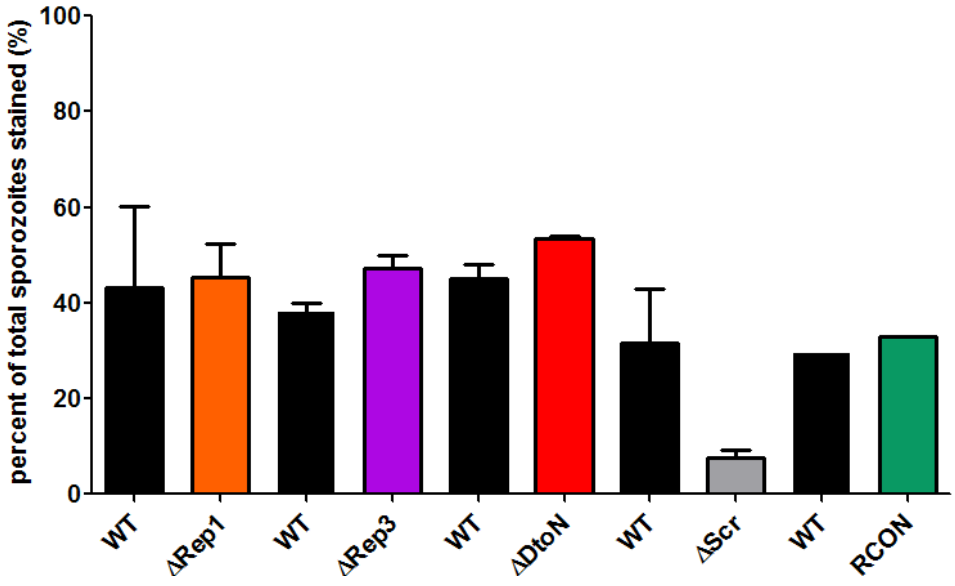

B)

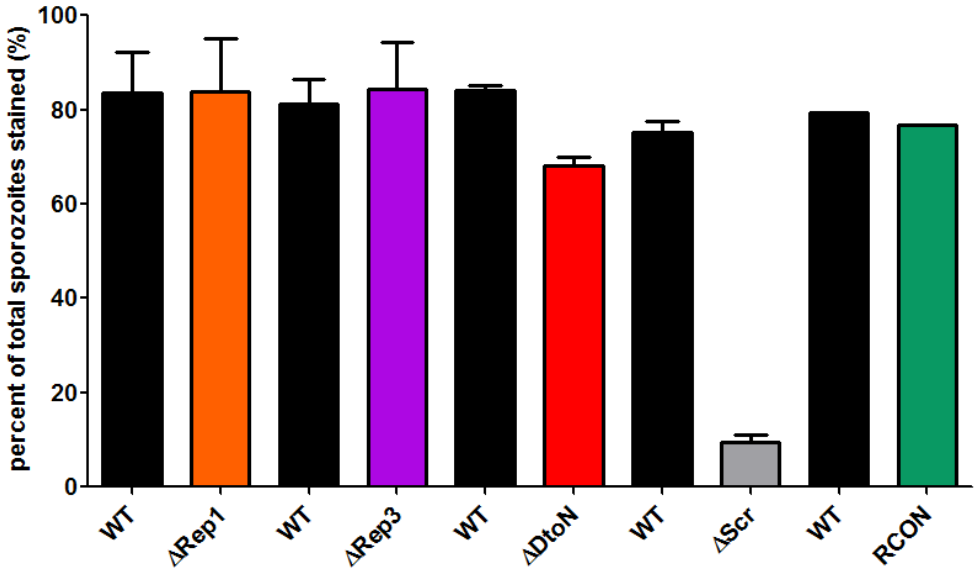

Fig. 22. Percent of mutant sporozoites that are stained compared to their WT controls in non-gliding and gliding conditions. A) Percent of TRAP stained sporozoites in non-gliding conditions. B) Percent of TRAP stained sporozoites in gliding conditions.

DISCUSSION

Here we provide evidence that motility phenotypes observed in WT and mutant sporozoites might be linked to TRAP secretion during gliding. We carried out IFAs of mutant sporozoites with a WT control in gliding and non-gliding conditions and stained the sporozoites with an antibody against TRAP. We categorized sporozoite staining patterns according to four categories: unstained, punctate staining, patch staining, and whole staining. After observing that the key differences in non-gliding and gliding sporozoites was between no stain and patch staining, with punctate and whole staining seen in lower numbers, we decided to group all punctate, patch, and wild type staining into a single category called 'stained'.

We consistently observed that in WT non-gliding sporozoites 55-65% of parasites are unstained and the remainder of sporozoites show some type of staining. This could mean that even in non-gliding conditions the sporozoites have begun to glide and release TRAP. There is a 40% range in the percent unstained WT sporozoites in non-gliding conditions. This is most likely due to handling differences in preliminary experiments and improved handling over time led to fewer sporozoites starting to glide before fixation. In order to address the concern that some sporozoites in non-gliding conditions are moving, the assay needs to be optimized. Future experiments to decrease gliding in non-gliding conditions are carrying out the initial stages of the assay in a cold room, fixing with PFA at 4°C, and fixing for 30 minutes instead of 1 hour to prevent transformation of the parasite. We would also change the centrifuge time settings so that sporozoites are immediately spun down onto coverslips without an acceleration or deceleration phase. Another aspect of the

assay that needs to be optimized is minimizing background staining due to mosquito debris. We have tried to address this by switching from a polyclonal α-TRAP to an IgG purified α-TRAP. Nevertheless, it is not clear if punctate staining is a consistently reliable indicator of TRAP secretion on the membrane; it is possible that some punctate staining may be due to background.

There was concern that 1 hour of gliding was too long and that sporozoites were dying so we carried out a side by side experiment comparing gliding between 20 mins and 1 hour. According to our data, we believe that continuing with 1 hour of gliding is a better option as the patch staining phenotype is more pronounced. If sporozoites are only allowed to glide for 20 mins, sporozoites might have less TRAP secretion and subtler phenotypes between mutants might not be observed. A future experiment that could be carried out in order to verify the whole staining patterns would be to carry out live/dead staining; this would allow us to observe whether whole staining is due to TRAP secretion while gliding or whether the sporozoites have died during the assay.

We saw significant changes in the percentages of stained WT sporozoites between non-gliding and gliding conditions suggesting that TRAP is only released from the micronemes and cleaved by the rhomboid protease when sporozoites start gliding. It is challenging to draw definite conclusions between WT and mutant sporozoites because so far we only have duplicates of our experiments. However, ΔRep1, ΔRep3, and RCon sporozoites seem to show similar percent stained to WT in gliding conditions. This corroborates live gliding and adhesion site turnover data from our lab and suggests that in these mutants, TRAP is deposited on the surface of the sporozoite when gliding occurs and

shed in a similar manner to WT. ΔDtoN seems to display slightly lower percent stained in gliding conditions than WT. This supports the subtle phenotypes seen in our live gliding and adhesion site turnover data where ΔDtoN sporozoites have a lower adhesion site turnover rate than WT. However, more replicates are required in order for us to have more confidence in the data.

The marked difference between ΔScr and WT TRAP staining in both non-gliding and gliding conditions could suggest that TRAP is not being secreted onto the surface of the sporozoite. When taken in the context of the previously described live gliding and adhesion site turnover data, it is possible that TRAP is not secreted in ΔScr due to the sporozoite attaching to the substrate but not being able to glide in a circular fashion. By carrying out primarily patch and wave gliding and not turning over as many adhesion sites, perhaps TRAP is unable to be distributed on the surface of the sporozoite and shed. It is also possible that the ΔScr sporozoites are attached to the substrate but not gliding at all, although this seems less likely due to the fact that the parasites are able to glide in live gliding assays. We intend to test ΔRep2 in future; if a similar pattern to ΔScr is seen in ΔRep2 (a mutant that is also shows patch and wave gliding and low adhesion site turnover), we would be able to have more confidence in our hypothesis that sporozoites first attach to the substrate and then initiate gliding and shedding of TRAP. In order to confirm that ΔScr does not lack TRAP, a future experiment where sporozoites are permeabilized needs to be carried out. This will both allow us to be sure that any TRAP staining phenotypes seen in ΔScr are not due to TRAP not being present in the micronemes of the sporozoite.

REFERENCES

[1] Almagro, J., and et al. 2014. Antibody Engineering & Therapeutics, The Annual Meeting of The Antibody Society. *Mabs.* 6:577.

[2] Amino, R., and et al. 2008. Host Cell Traversal Is Important for Progression of the Malaria Parasite through the Dermis to the Liver. *Cell Host and Microbe.* 3:88.

[3] Amino, R., and et al. 2006. Quantitative imaging of Plasmodium transmission from mosquito to mammal. *Nature Medicine.* 12:220.

[4] Amino. R., and et al. 2007. Imaging malaria sporozoites in the dermis of the mammalian host.. *Nature Protocol.* 2:1705.

[5] Balaban, A. 2017. Sporozoite gliding and motility data. Unpublished data.

[6] Bane, K., and et al. 2016. The Actin Filament-Binding Protein Coronin Regulates Motility in *Plasmodium* Sporozoites. *PLOS Pathogens.* 12.

[7] Baum, J. 2005. A Conserved Molecular Motor Drives Cell Invasion and Gliding Motility across Malaria Life Cycle Stages and Other Apicomplexan Parasites*. *J. Biol. Chem.* 281:5197.

[8] Coppi, A., and et al. 2011. The malaria circumsporozoite protein has two functional domains, each with distinct roles as sporozoites journey from mosquito to mammalian host. *Jem.* 208:341.

[9] Coppi, A., and et al. 2005. The Plasmodium circumsporozoite protein is proteolytically processed during cell invasion. *Jem.* 201:27.

[10] Cowman, A. 2016. Malaria: Biology and Disease. *Cell.* 167:610.

[11] Ejigiri, I., D. Ragheb, and et al. 2012. Shedding of TRAP by a Rhomboid Protease from the Malaria Sporozoite Surface Is Essential for Gliding Motility and Sporozoite Infectivity. *PLOS Pathogens.* 8.

[12] Ejigiri, I., and P. Sinnis. 2009. Plasmodium sporozoite–host interactions from the dermis to the hepatocyte. *Current Opinion in Microbiology.* 12:401.

[13] Ferguson, D., A. Balaban, and et al. 2014. The Repeat Region of the Circumsporozoite Protein is Critical for Sporozoite Formation and Maturation in Plasmodium. *Plos One.* 9.

[14] Hopp, C., and et al. 2015. Longitudinal analysis of *Plasmodium* sporozoite motility in the dermis reveals component of blood vessel recognition. *Elife.* 4.

[15] Hopp, C., and P. Sinnis. 2015. The innate and adaptive response to mosquito saliva and *Plasmodium* sporozoites in the skin. *Ann. NY. Acad.* 1342:37.

[16] Kester, K., et al. 2001. Efficacy of Recombinant Circumsporozoite Protein Vaccine Regimens against Experimental *Plasmodium falciparum* Malaria. *J Infect Dis.* 183: 640.

[17] Lee E., and et al. 2014. Complete humanization of the mouse immunoglobulin loci enables efficient therapeutic antibody discovery. *Nature Biotechnology.* 32:356.

[18] Long, C., and F. Zavala. 2016. Malaria vaccines and human immune responses. *Current Opinion in Microbiology.* 36:96.

[19] Menard, R. 2000. The journey of the malaria sporozoite through its hosts: two parasite proteins lead the way. *Microbes and Infection.* 2:633.

[20] Mota, M., and et al. 2001. Migration of Plasmodium Sporozoites Through Cells Before Infection. *Science.* 291:141.

[21] Myung, J., and et al. 2004. The Plasmodium circumsporozoite protein is involved in mosquito salivary gland invasion by sporozoites. *Molecular & Biochemical Parasitology.* 133:53.

[22] RTS,S Clinical Trials Partnership 2014. Efficacy and Safety of the RTS,S/AS01 Malaria Vaccine during 18 Months after Vaccination: A Phase 3 Randomized, Controlled Trial in Children and Young Infants at 11 African Sites. PLoS Medicine.

[23] Sawasaki, T., and et al. 2002. A cell-free protein synthesis system for high-throughput proteomics. *Pnas.* 99:14652.

[24] Stewart, M., and J. Vanderberg. 1988. Malaria Sporozoites Leave Behind Trails of Circurnsporozoite Protein During Gliding Motility. *J. Protozol.* 35:389.

[25] Stoute, J.A., and et al. 1998. Long-Term Efficacy and Immune Responses following Immunization with the RTS,S Malaria Vaccine. *Journal of Infectious Disease.* 178:1139.

[26] Sultan, A., V. Thathy, and et al. 1997. TRAP is Necessary for Gliding Motility and Infectivity of Sporozoites. *Cell.* 90:511.

[27] Tomas, A., and et al. 2001. P25 and P28 proteins of the malaria ookinete surface have multiple and partially redundant functions. *The EMBO Journal.* 20:3893.

[28] Vanderberg, J., and U. Frevert. 2004. Intravital microscopy demonstrating antibody mediated immobilisation of *Plasmodium berghei* sporozoites injected into skin by mosquitoes. *International Journal for Parisitology.* 34:991.

[29] VanBuskirk, K.; Mikolajczak, SA. et al. 2011. Disruption of the Plasmodium falciparum liver-stage antigen-1 locus causes a differentiation defect in late liver-stage parasites. Cell Microbiol. 13: 1250.

[30] Vaughan, A., S. Kappe, and et al. 2012. Development of humanized mouse models to study human malaria parasite infection. *Future Microbiol.* 7.

[31] Yamauchi, L., and et al. 2007. Plasmodium sporozoites trickle out of the injection site. *Cell Microbiology.* 9:1215.

CURRICULUM VITAE

Natasha Vartak

DOB: 09/26/1992 natasha.vartak1@gmail.com
Place of Birth: Kettering, U.K.

Education

Johns Hopkins Bloomberg School of Public Health Baltimore, MD
Masters of Science, Biochemistry and Molecular Biology, expected May 2017

State University of New York at Geneseo Geneseo, NY
Bachelor of Science, Biochemistry, May 2015
Minor in Mathematics

Professional Experience

Johns Hopkins Bloomberg School of Public Health Baltimore, MD
Malaria Research Institute, *Researcher*
January 2016 – present

- Biological research to investigate the motility of *Plasmodium*

Access Opportunities Programs at SUNY Geneseo, *Tutor* Geneseo, NY
October 2012 – May 2013

- Guided Access Opportunities Programs students in the instruction of introductory Biology and Chemistry

Volunteering and Leadership Experience

Community Adolescent Sexual Education (CASE), *Educator* Baltimore, MD
September 2015 – April 2016

- Created lesson plans and taught sexual education classes to 7th grade students in a Baltimore city school

Teresa House Comfort Care Home, *Volunteer* Geneseo, NY
February 2014 – April 2015

- Provided care and company for residents living at Teresa House hospice

Posters and Theses

Natasha Vartak. 'Investigating the Motility of *Plasmodium*'. Masters of Science thesis. April 2016.

Natasha Vartak, Amanda E. Balaban, and Photini Sinnis. 'Development of a fluorescence intensity assay to assess gliding motility of *Plasmodium* sporozoites'. Johns Hopkins Malaria Research Institute Malaria Day. April 2017.

Natasha Vartak. 'The Activity of IL-17/IL-17R in Colon Cancer and Breast Cancer'. Master of Health Science thesis. May 2016.